



This is the accepted version of this article. Published as:

Frost, Ray L. and Zbik, Marek (2010) *PDMS spreading morphological patterns on substrates of different hydrophilicity in air vacuum and water*. *Journal of Colloid and Interface Science*, 344(2). pp. 563-574.

© Copyright 2010 Elsevier

1 **Polydimethylsiloxane (PDMS) spreading morphological patterns on**
2 **silicon wafers in vacuum and in air**

3

4 **Marek S. Żbik and Ray L. Frost***

5

6 *Inorganic Materials Research Program, School of Physical and Chemical Sciences,*
7 *Queensland University of Technology 2 George Street, GPO Box 2434, Brisbane Qld*
8 *4001 Australia.*

9

10 **Corresponding Author: Ray L. Frost**

11 **Email: r.frost@qut.edu.au**

12 **P: +61 7 3138 2407**

13 **F: +61 7 3138 2407**

* Author for correspondence (r.frost@qut.edu.au)

14 **Polydimethylsiloxane (PDMS) spreading morphological patterns on**
15 **silicon wafers in vacuum and in air**

16

17 **Marek S. Żbik and Ray L. Frost***

18

19 *Inorganic Materials Research Program, School of Physical and Chemical Sciences,*
20 *Queensland University of Technology 2 George Street, GPO Box 2434, Brisbane Qld*
21 *4001 Australia.*

22

23

24 **Abstract:**

25

26 This paper reports the investigation of the morphological patterns and kinetics of
27 polydimethylsiloxane (PDMS) spreading on a silicon wafer using combination of
28 techniques including ellipsometry, atomic force microscope (AFM), scanning electron
29 microscope (SEM) and optical microscopy. A macroscopic silicone oil drops as well
30 as PDMS water based emulsions were studied after deposition on a flat surface of a
31 silicon wafer in air, water and vacuum. Measurements using an imaging ellipsometer
32 clearly show the presence of a precursor film. The diffusion constant of this film,
33 measured with a 60 000 cS PDMS sample spreading on a hydrophilic silicon wafer, is
34 $D_f = 1.4 \times 10^{-11} \text{ m}^2/\text{s}$. Regardless of their size, density and method of deposition,
35 droplets on both types of wafer (hydrophilic and hydrophobic) flatten out over a
36 period of many hours, up to 3 days. During this process neighbouring droplets may
37 coalesce, but there is strong evidence that some of the PDMS from the droplets
38 migrates into a thin, continuous film that covers the surface between droplets. The
39 thin film appears to be ubiquitous if there has been any deposition of PDMS.
40 However, this statement needs further verification. One question is whether the film
41 forms immediately after forced drying, or whether in some or all cases it only forms
42 by spreading from isolated droplets as they slowly flatten out.

43

44 **Keywords:** polydimethylsiloxane, Silicone oil, Spreading, contact angle.

45

* Author for correspondence (r.frost@qut.edu.au)

46 1. Introduction

47

48 Spreading of silicon oil on various surfaces is of importance to many industrial
49 applications and especially in cosmetic industries where silicon oil is widely used. To
50 study the spreading dynamics, simplified conditions are often used in wetting
51 experiments. Flat and atomically smooth solid surfaces and non-volatile liquids are
52 preferable. A smooth surface is necessary to avoid hysteresis effects and in practice a
53 silicon wafer with highly polished surface (inevitably with a thin layer of oxide) is a
54 convenient choice. Using polydimethylsiloxane (PDMS) as a pure and non-volatile
55 liquid minimises possible Marangoni effects driven by evaporation. PDMS is
56 available with a wide range of molecular weights, giving a wide range of viscosity
57 (η). The silicon wafer/PDMS combination was the popular choice for a range of
58 experimental studies to be described below that were carried out in the late 1980's,
59 with French researchers at the forefront.

60

61 Spreading a PDMS droplet onto a solid surface belongs to a “dry” wetting
62 processes because of the non-volatility of the liquid. Because the shape of the droplet
63 deposited on flat surface depends on the droplet size we concentrate here on small
64 droplets where $R \ll \kappa^{-1}$ (κ^{-1} is the capillary length), in which regime the effects of
65 gravity are negligible. In such case, the long range capillary forces play the crucial
66 role in determining the contact line between solid and liquid. This force pulls out of
67 the drop a film whose thickness results from a balance between the large capillary
68 term and large disjoining pressure [1], and the extent of the film can be macroscopic.
69 The spreading and thin-film dynamics of the precursor film have been the subject of a
70 number of theoretical [2-3] and experimental [4-10] papers. The profile of the
71 macroscopic droplet is measured using interference microscopy [11] but thickness of
72 the precursor film is experimentally measured using ellipsometry [5, 8]. At
73 equilibrium, the film is a “pancake” [12] of thickness e , with microscopic contact
74 angle $\pi/2$, owing to the thickening influence of the disjoining pressure. According to
75 [1], the width ΔR of the foot can be written as

76

$$\Delta R = \sqrt{(D_f t)} \quad (1)$$

77 where D_f is a diffusion coefficient for the foot and t is time. As long as the volume
78 of the foot is negligible, the central drop and the foot behave independently. The
79 diffusion coefficient for the foot is also found to depend on the roughness amplitude h
80 and on the fluid viscosity η :

$$81 \quad D_f \sim h/\eta \quad (2)$$

82 The shape of the macroscopic drop is rather smooth, without steps being observed
83 in the precursor film profile.

84

85 The aim of the research described in this paper is to investigate the morphological
86 patterns and kinetics of PDMS spreading on silicon wafer using combination of
87 techniques like ellipsometry, atomic force microscope (AFM), scanning electron
88 microscope (SEM) and optical microscopy. A macroscopic silicone oil drops as well
89 as PDMS water based emulsions were studied after deposition on a flat surface of
90 silicon wafer in air, water and vacuum.

91

92

93 **2. EXPERIMENTAL DETAILS**

94

95 Sample used was bulk silicon oil (Down Corning) of viscosity 60,000 cS used for
96 spreading experiments in an imaging ellipsometer, optical microscopy and scanning
97 electron microscopy (SEM). The others are emulsion samples, one with 10 μm
98 droplets of 60,000 cS PDMS (Unilever sample DC2-1310 BB), and six emulsions
99 with 50% v/v of 1 μm PDMS droplets stabilised by a non-ionic surfactant. The
100 viscosities of the PDMS in these six samples, numbered 1 through 6, are 20, 350,
101 5000, 60000, 300000 and 600000 cS respectively.

102

103 An Imaging Ellipsometer (Beaglehole Instruments, New Zealand) was used to
104 investigate thin films of PDMS on a silicon wafer. The main feature of this particular
105 ellipsometer is that it takes an image, capturing the thickness data over an area of the
106 sample. The incident light beam was filtered by optical 600nm wave length filter.
107 Resolution is $\sim 10 \mu\text{m}$ in directions parallel to the surface, and $\sim 0.1 \text{ nm}$ in the normal
108 (i.e. film thickness) direction.

109 The SEM studies were carried out using a Philips XL30 field emission gun
110 microscopy operating at 5 kV accelerating voltage. Studied samples were not coated
111 and observe in the vacuum 10^{-5} millibars over 20 hours. A Nanoscope III AFM
112 (Digital Instrument) was used for oil droplet imaging in tapping mode with scan head
113 J(100 x 100 μm) and scan rate 0.5 – 1 Hz.

114

115 Imaging ellipsometry images were taken of macroscopic drops of 60,000 cS
116 PDMS deposited on silicon wafers. The wafers were cleaned with chromic acid,
117 distilled water and ethanol, then treated in a water-vapour plasma, which means that
118 their surfaces are hydrophilic with contact angle ~ 0 . Very small drops (>1 mm) were
119 deposited in air by dipping a sharp tweezers tip into PDMS and touching the drop to
120 the wafer surface.

121

122 **3. Results and discussion**

123

124 3.1. Imaging ellipsometry of the PDMS precursor film

125

126 All AFM, ellipsometer and SEM images show distinctive aurora spreading around
127 macroscopic oil drop but do not directly show the film thickness. Software available
128 on ellipsometer can correctly compute the thickness at a single point in the image, and
129 an alternative software program that uses an analytical expression to compute
130 thicknesses at every point in the image. We also have made a semi-empirical
131 calculation which should be reasonably accurate for films of PDMS that are less than
132 a few nm thick. Applying that to the area maps of (x,y) data produces an area map of
133 the film thickness d . This map shows the extent of spreading of a precursor film, and
134 also delineates the perimeter of the macroscopic drop.

135

136 Optical microscopy in monochromatic line shows a series of Newton's rings that
137 can be used to estimate the height and contact angle of the macroscopic drop.
138 Although these methods have not been combined for the drops shown below, in
139 principle such a combination should show the profiles of both the macroscopic drop
140 and the precursor film.

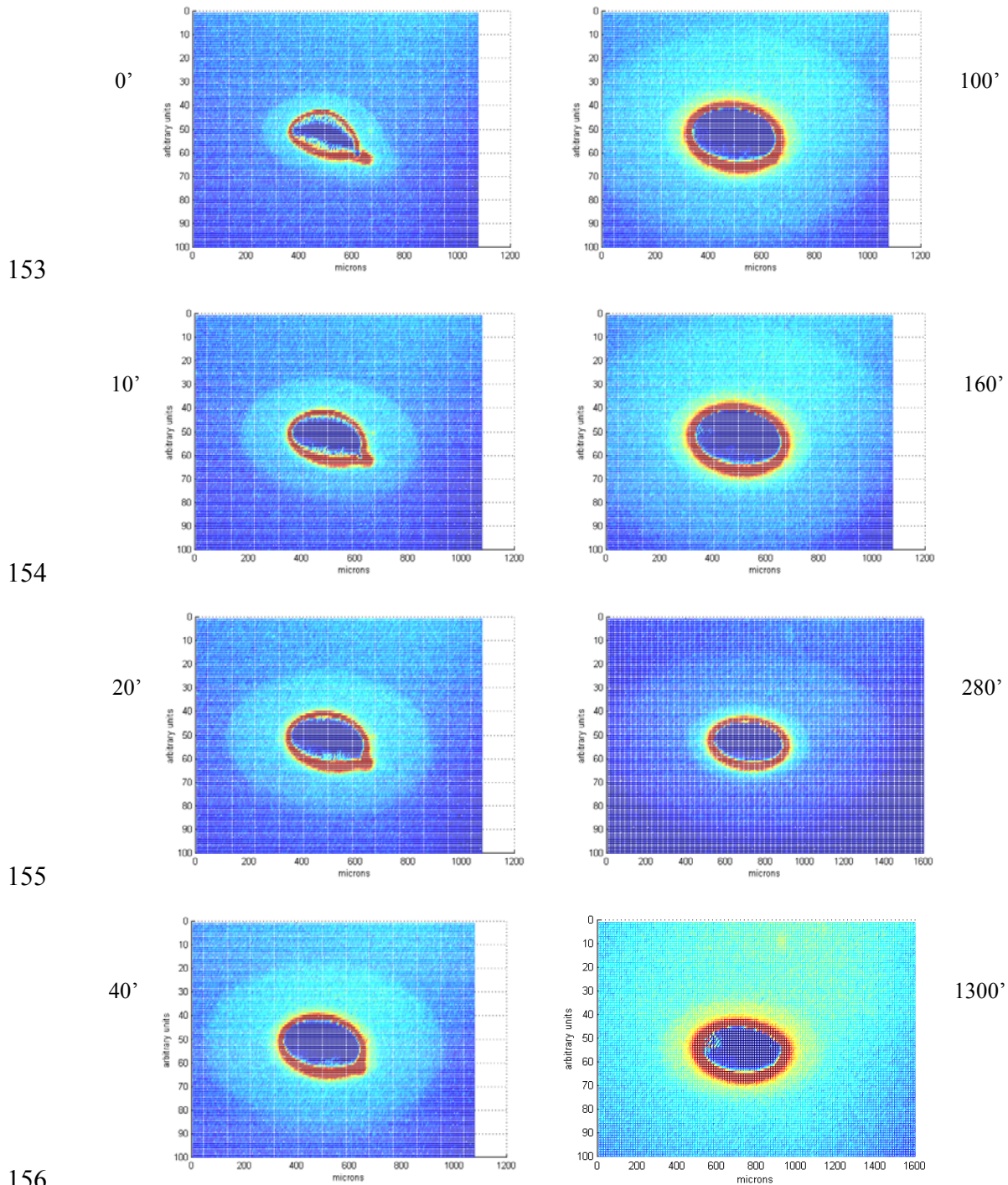
141

142 Figure 1 shows the thickness maps for a single drop, taken at various times after
143 deposition. The elapsed time in minutes is shown beside each image. Note that the

144 images are foreshortened because they are viewed at a large angle of incidence (65°
145 from the perpendicular – this angle gives good resolution in the ellipsometric
146 parameters). Hence the horizontal axis shows a true lateral dimension, but the vertical
147 axis in these figures is not calibrated (the numbers shown are simply camera pixels).
148 Furthermore, due to the high angle of incidence, only the central horizontal region of
149 the sample is in proper focus. Note also that the scale is different for the last two
150 images which were recorded at a lower magnification.

151

152



157 **Fig. 1.** Thickness maps surrounding a PDMS drop deposited on the plasma cleaned silicon wafer.

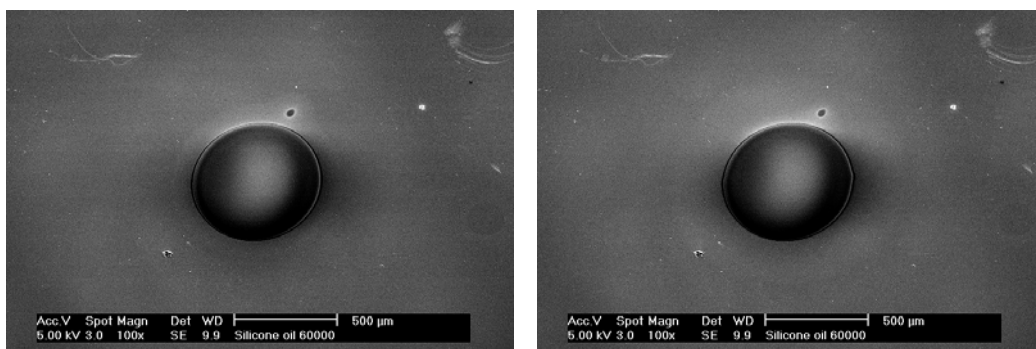
- 159 Several features are immediately apparent from the series of thickness maps in Fig. 1:
- 160 1. There is a precursor film spreading ahead of the drop, which continues to
 161 spread over a period of hours. This is seen as the pale blue annulus around the
 162 drop, whose macroscopic edge appears as yellow (going to dark red as its
 163 thickness increases). Our measurements show that the precursor film thickness

164 is $d \approx 0.5$ nm. For the first four hours the thickness of the precursor film
165 appears to diminish as it spreads, but it is difficult to be certain about this
166 because the ellipsometer measurements may vary slightly over this period of
167 time, and comparing the calculations between different images may not be
168 precise at the 0.1 nm level.

169 2. The main drop spreads slightly and slowly, and becomes more circular as it
170 spreads.

171 3. In the final image taken the following day (after 1300 min), part of the drop
172 appears to have spread into the precursor film, thickening it to 1-2 nm.

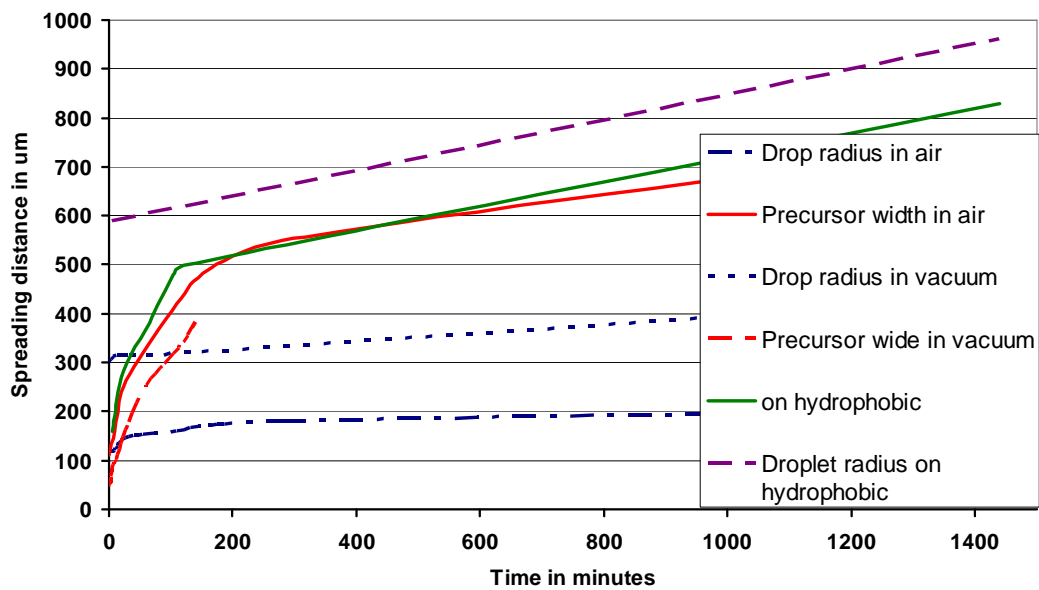
173 The development of precursor layer was also observed on the plasma cleaned (low
174 contact angle) silicon wafer in vacuum chamber of SEM. In SEM micrographs
175 presented in Fig. 2 two different in size droplets have been observed. Larger droplet,
176 0.6 mm in diameter has very small, only 25 μm in diameter satellite micro-droplet.
177 The precursor layer can be seen on SEM images as distinctive light aurora spreading
178 from both droplets. Because precursor forms immediately after droplet deposition and
179 handling sample into SEM chamber with subsequent air evacuation take few minutes
180 it is impossible to observe development of precursor film layer from the very
181 beginning. In Fig. 2a precursor film already spreads 100 μm from macroscopic
182 droplet foot. Interestingly the width of spreading film seems to be independent of the
183 macroscopic droplet size and is equal in size for larger and smaller droplets. SEM
184 measurements gave possibility to measure the rate of spreading the precursor film but
185 gave no indication about thickness of this film unlike ellipsometry did.



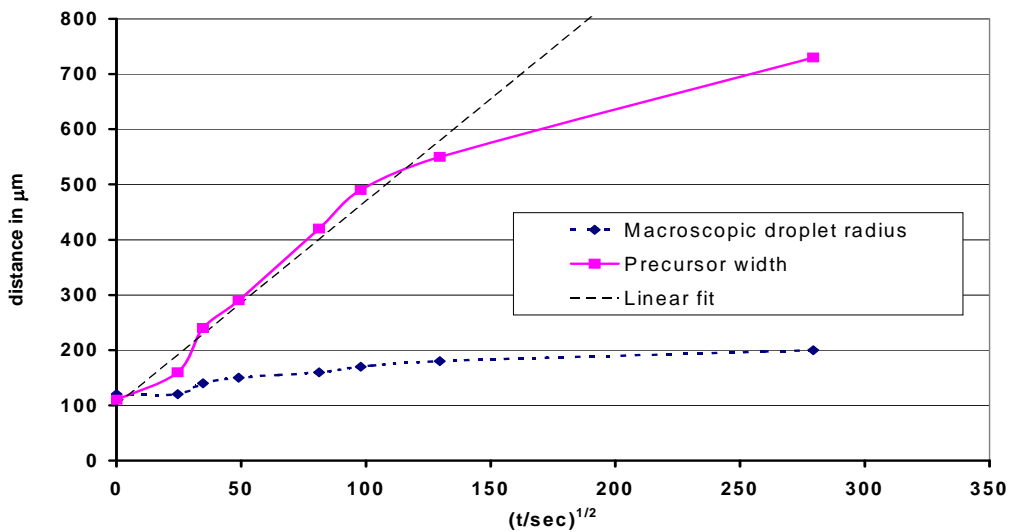
186
187 **Fig. 2.** SEM micrograph of silicon oil drop at the beginning of the experiment and after one hour.
188 Bright ring of precursor film evolve.

189

190 Both precursor film widths measured in function of time, spread on plasma
 191 cleaned silicon wafer in air (using ellipsometry) and in vacuum (using SEM) are
 192 shown in graph Fig. 3. This figure shows the radius of the main drop and width of the
 193 precursor film (measured from the edge of the drop to its periphery) as a function of
 194 time. From curves in Fig. 3 is clear that spreading rate of the precursor film is similar
 195 regardless of hydrophilicity of substrate in air and vacuum which indicate similar
 196 slope angle.
 197



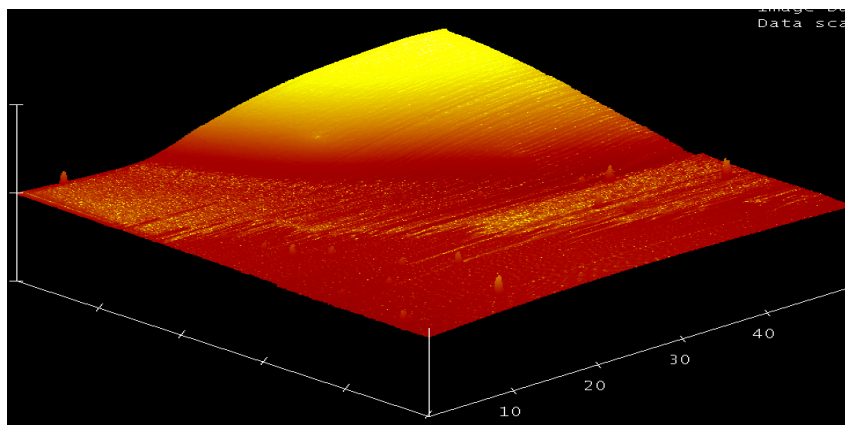
198
 199 **Fig. 3.** Increase of drop radius and precursor film width with time, estimated from the images in Figs.
 200 1 & 2. The upper plot has time on a linear scale; the lower one compares precursor film width to \sqrt{t} .



201
 202

203 **Fig. 4.** Increase of drop radius and precursor film width with time, estimated from the images in Fig.
204 1. The upper plot has time on a linear scale; the lower one compares precursor film width to \sqrt{t} .
205

206 Plotting the precursor film width against the square root of time (Fig 4, lower part)
207 shows linear behaviour at least for the first four hours. The slope of this line
208 corresponds to a precursor film diffusion constant (from equation (1)) of $D_f = 1.4 \times$
209 $10^{-11} \text{ m}^2/\text{s}$. $t = 0$ was set when the first measurement was taken, not when the drop
210 was deposited. Extrapolating the straight line back to zero precursor film width is
211 consistent with a delay of about 12 minutes between drop deposition and the first
212 recorded image. Ellipsometry measurements for both precursor films formed in air
213 and in vacuum have similar thickness 2.7 nm on top of the oxide layer estimated as
214 1.4 nm in thickness.
215

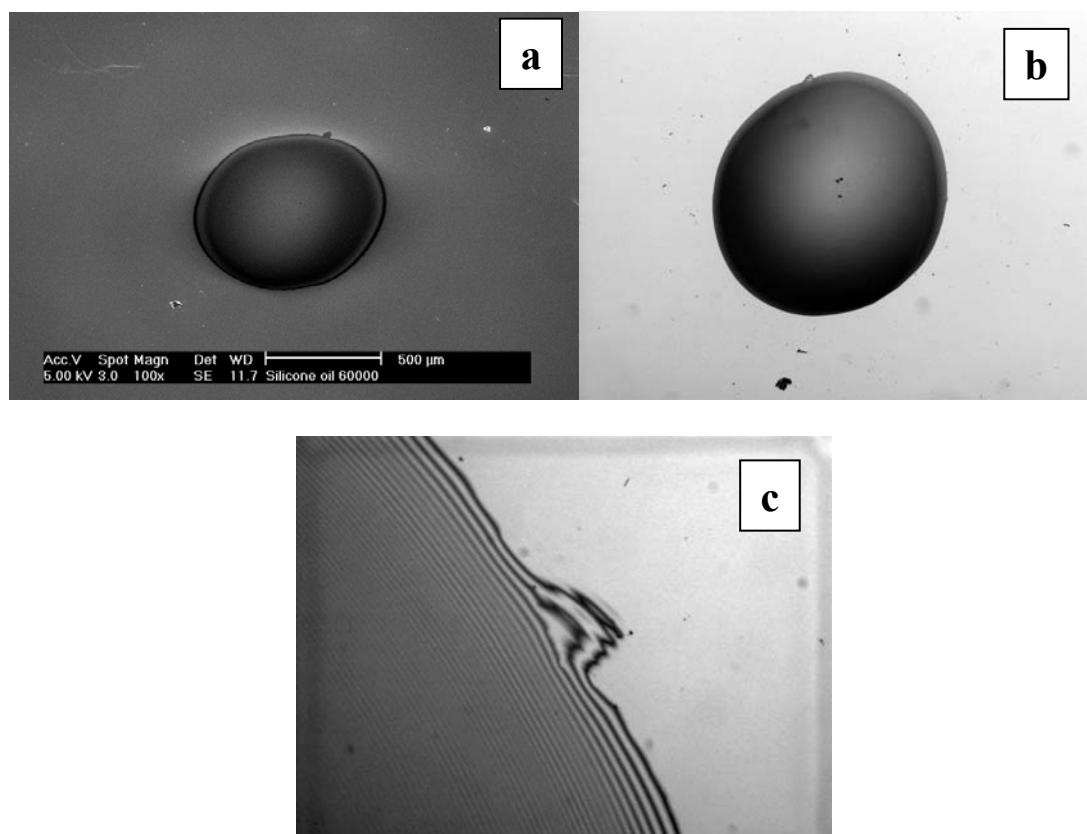


216
217 **Fig. 5.** AFM 3-dimensional image of macroscopic droplet with possible precursor film advancing
218 around its perimeter.
219

220 It is very difficult to observe the precursor film development using AFM partly
221 because soft oil droplet surface forms film which is in the same magnitude with
222 silicon wafer roughness. Fig. 5 showing 3-dimensional reconstructions of AFM
223 images, a precursor film extending up to 20 micrometres can be seen. The thickness
224 of this precursor foot measured near the border of a macroscopic droplet, from the
225 section of this droplet is about 13 nm which is many (about 18) times the size of a
226 molecular monolayer. However, the front of the precursor film may be further from
227 what we can observe in AFM micrographs and the real extent may be larger.
228

229 In Fig. 6a the edge of the macroscopic silicon oil drop placed in vacuum observed
230 after overnight (18 h since deposition Fig. 2) reach the small droplet perimeter and
231 both droplets are merging. This process also has been observed in optical microscopy
232 in Fig. 6b. Estimating from Newtonian rings in small droplets seen in monochromatic
233 light 589.5 nm on magnified fragment in Fig. 6c the high of this droplet is about 412
234 nm.

235



236
237

238
239

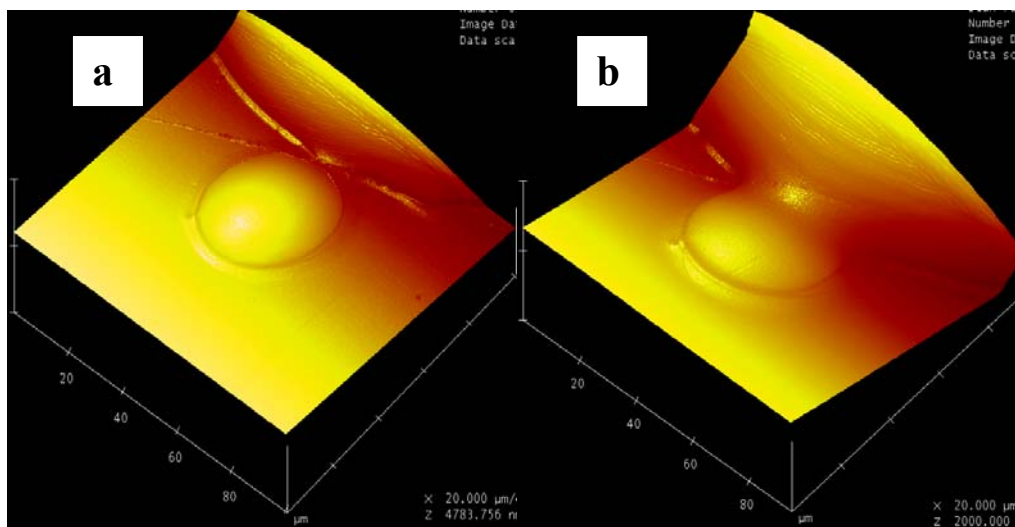
240 **Fig. 6.** SEM (a) and optical microscopy observations (b – white light and c- monochromatic light) of
241 merging oil droplets which differ in size.

242

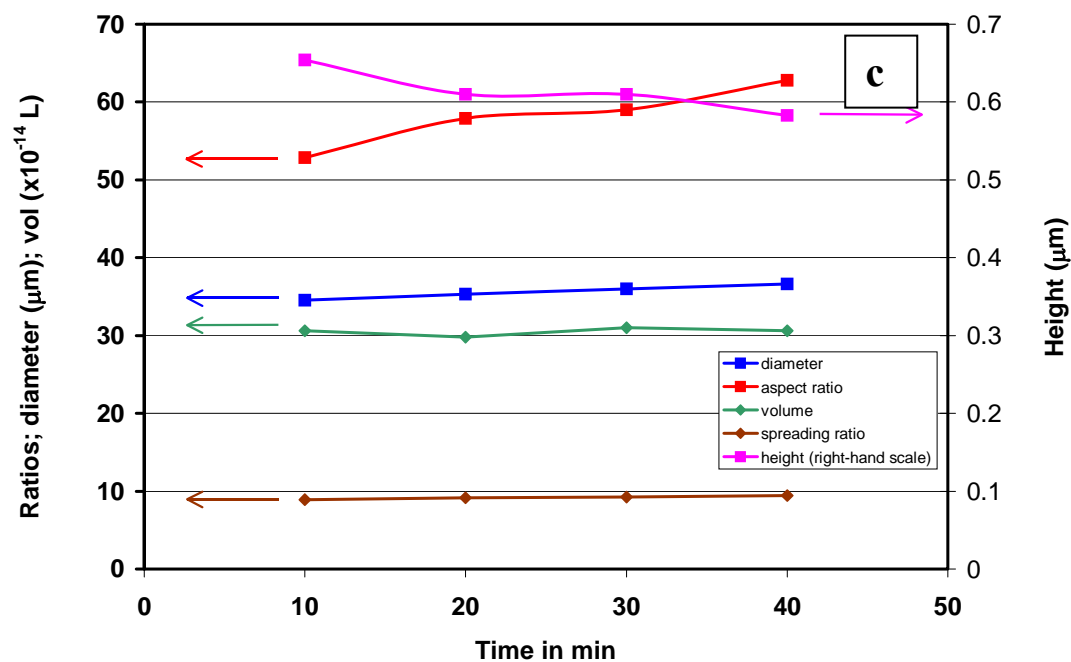
243 Merging oil droplets also has been observed using AFM presented in Fig. 7 at the
244 beginning of observation (Fig. 7a) and its final stage after 100 min (Fig. 7b). Also in
245 this occasion droplets largely differ in size. Images from intermediate times in this
246 series were analysed for the dimensions change of the small drop. These parameters
247 are displayed in Fig. 7c and show steady spreading with a slow increase in diameter
248 (less than 0.1 μm per minute) and a progressive decrease in height. The droplet
249 volume, calculated from its dimensions and assuming the shape is a spherical cap,
250 remains steady, while the aspect ratio (the ratio of diameter to height of the spreading
251 drop) increases as the drop flattens. The “spreading ratio” (the ratio of drop diameter

252 on the surface to the calculated diameter of a spherical drop of the same volume) is
 253 about 2 in this case, and increases slowly with time.

254



255
 256



257
 258 **Fig. 7.** AFM 3-dimensional images showing the gradual coalescence of a small silicone drop with a
 259 large one. Image b was taken 100 minute after image a have been recorded. The area is 100 μm × 100
 260 μm. © The time evolution of shape parameters of the small drop taken from Figure 7c.

261

262 **OBSERVATIONS USING OPTICAL MICROSCOPY**

263

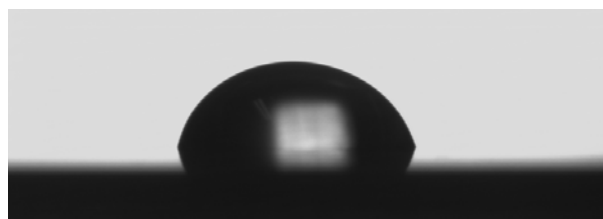
264 It is simple to observe the spreading of a macroscopic drop using optical
 265 microscopy. This can be done with a standard vertically-mounted microscope, in
 266 which case the drop can be illuminated with monochromatic light, and Newton's rings

267 used to determine the drop profile and height. Alternatively, a more direct image of
268 drop profile is obtained using a low-power horizontal microscope designed for
269 measuring contact angles of sessile drops. Drops can be monitored over a period up to
270 many days if necessary, and it is straightforward to make similar observations under
271 water. The precursor film is too thin to be observed by optical microscopy.

272

273 Figure 8 presents a series of optical micrographs taken in the horizontal
274 configuration, showing profiles of a PDMS large macroscopic drop during its
275 spreading on a silicon wafer in air. It is clearly seen that the drop spreads, reducing its
276 contact angle and height, over a period of hundreds of minutes. The diameter of the
277 drop at 1 minute (this is the time after deposition of the drop) is 3.3 mm. For clarity of
278 picture we show in Fig. 8 only three photograph of the first, intermediate and last
279 stage of drop spreading.

280



1 min

281

282

283



36 min

284

285

286

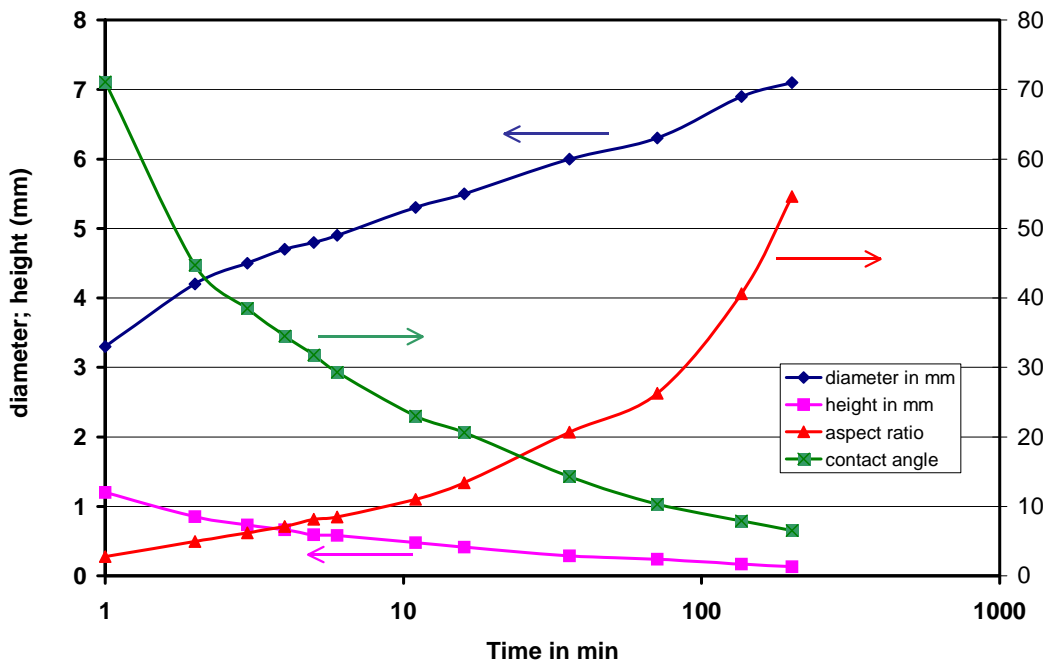


201 min

287

288

289



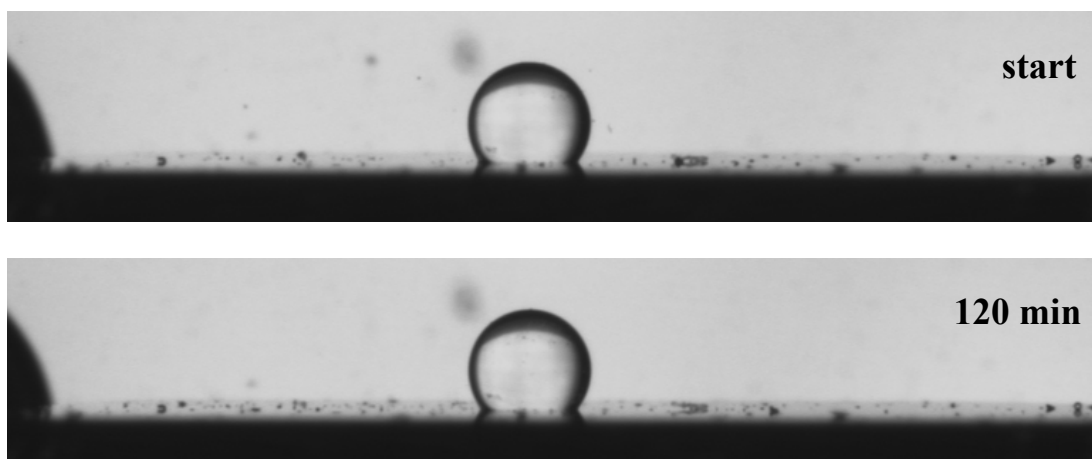
290

291 **Fig. 8** Optical micrographs of a silicone drop spreading on a silicon wafer in air. Shape analysis of
 292 the optical images from, showing the spreading and flattening of the drop. Note the large decrease in
 293 contact angle from 70° to less than 10° over 200 minutes for this 60,000 cS silicone on silicon in air.
 294

295 Figure 8 shows the change in dimensions of the spreading drop illustrated in
 296 profiles photographs, i.e. spreading on a silicon wafer in air. The drop diameter on the
 297 surface increases while its height decreases, thus the contact angle decreases and the
 298 aspect ratio increases quite markedly. The volume is calculated as 6 mL and the
 299 spreading factor is 4.

300 In contrast to this, Fig. 9 shows that a PDMS droplet (0.7mm in diameter) under
 301 water does not spread measurably on the silicon wafer over a similar time frame.

302



303
 304

305
 306

307 **Fig. 9** Optical images of a 0.7 mm diameter silicone drop on a silicon wafer under water, showing
 308 that in this environment it does not spread, over a time frame similar to that of Fig. 8.
 309

310 The advancing and receding contact angles of water on the silicon wafer has been
 311 measured using sessile drops apparatus and gives values of 63° and 25° respectively.

312 In Figure 10 there is an interesting observation of how water spreads on a wafer
 313 that was previously covered in silicone oil. Fig 10A shows the low receding contact
 314 angle of water on top of a thin PDMS layer, giving a low value of about 15°. The
 315 water droplet shown in Fig. 10B was placed on top of a thick PDMS film, and shows
 316 an unusual shape. Close examination shows a slight groove running around the drop
 317 at about 1/3 of its height, which may be a PDMS/water/air three-phase line at the top
 318 of a PDMS meniscus rising up the water drop, as illustrated schematically in Fig.
 319 10C.

320

321

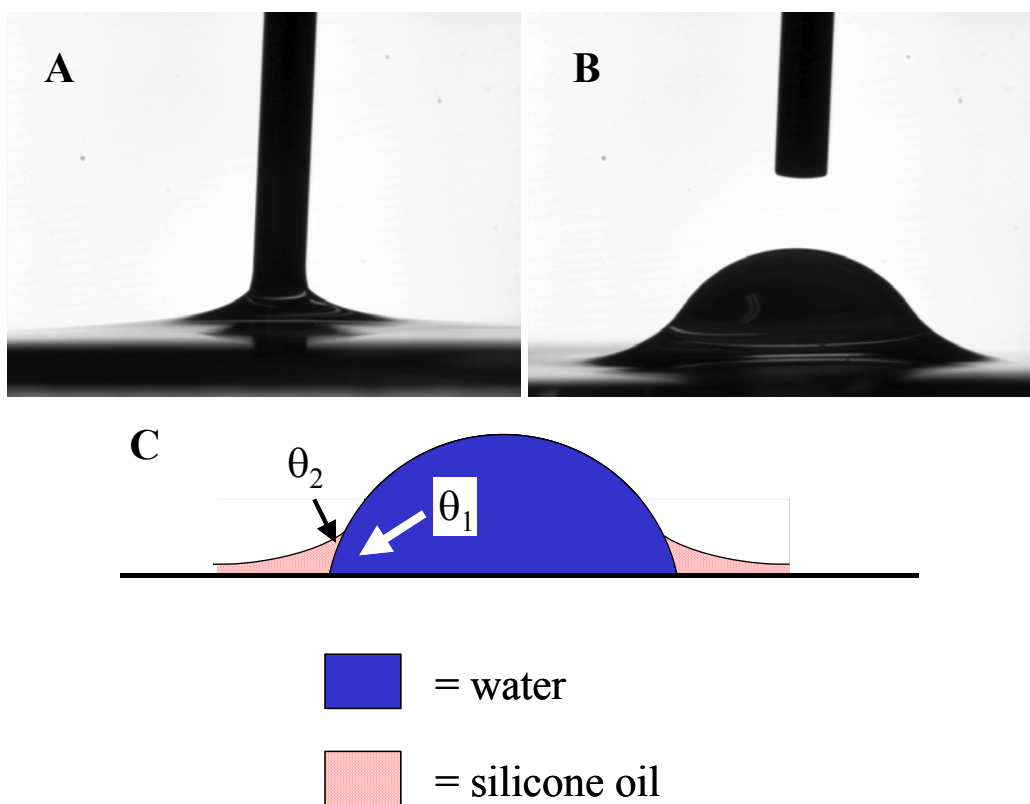


Fig. 10. Optical images of a water drop pressed onto a silicon wafer that was previous covered with a thin (A) or thick (B) layer of silicone oil. The syringe diameter is 1 mm. In (B) a faint, roughly horizontal, line can be seen about 1/3 of the way up the drop on the left-hand side. We think this is a silicone/water/air three-phase line as illustrated schematically in (C), where θ_1 is the contact angle of water on silicon underneath silicone oil, and θ_2 is the contact angle of silicone oil on water in air.

2. METHODS USED TO DEPOSIT PDMS DROPLETS FROM EMULSIONS

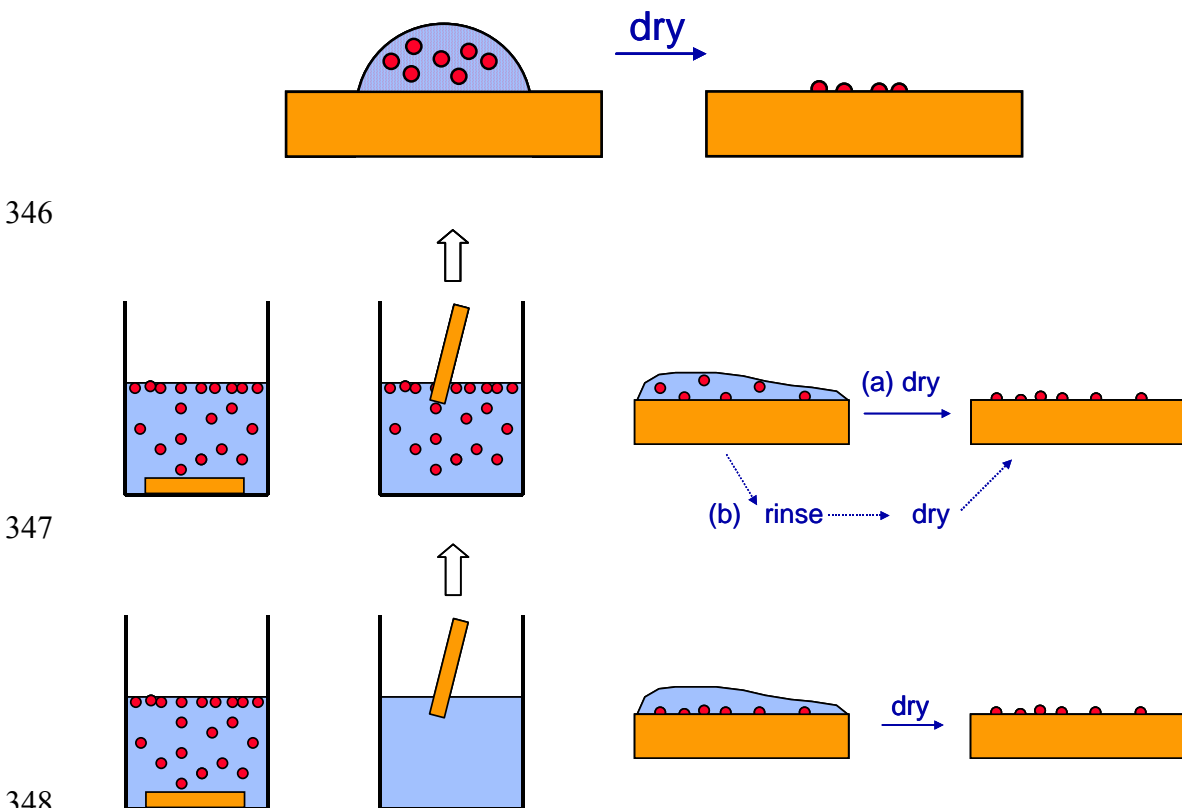
Four different methods were used for deposition of PDMS emulsion droplets onto flat solid substrates. They were not all successful, as it was shown below, but the

336 information gained by trying different methods has proven helpful in understanding
337 how deposition may be achieved using this emulsion.

338

339 The various methods are illustrated in Figure 11. The first method is to place a
340 macroscopic drop of the diluted emulsion form concentrated (50%) one by a factor of
341 $\sim 10^3$ to 10^4 , directly onto a wafer placed horizontally. The drop is then dried on air, or
342 placing in a vacuum chamber. For most of the results shown below, and unless stated
343 otherwise, the vacuum drying method was used since it gave the least amount of
344 mechanical disturbance caused by fluid flow during drying.

345



346

347

348

349

350

351 **Fig. 11.** Illustrating the three methods to test deposition of emulsion drops onto a flat solid substrate.
352 In Method 1 (top) a drop of emulsion is placed on a horizontal substrate and then dried. In Method 2a
353 (middle) the substrate is immersed in the emulsion for several minutes, withdrawn and then dried. A
354 variation (2b) is to rinse the suspension from the wafer after withdrawal and before drying. Method 3
355 (bottom) is similar to the second, except that substrate is immersed in pure water and subsequently
356 emulsion is produce by addition of concentrated emulsion droplets, latter is diluted by copious
357 amounts of water before withdrawing the substrate and drying it.

358

359 The second method (Method 2a) consists of immersing the substrate in a diluted
360 suspension of emulsion drops for about one minute, then withdrawing it and drying it
361 in vacuum. The third method (2b) is a variation on this in which the suspension that is

362 entrained on withdrawing the substrate is rinsed by water before drying. This is
363 designed to test whether droplet deposition occurs before the drying process.

364
365 The final method (Method 3) starts by immersing the substrate in pure water, then
366 produce suspension by addition of concentrated PDMS emulsion to water vessel with
367 substrate lying on the bottom. However, before withdrawing the substrate, the
368 suspension is washed away by repeated replacement by water. This variation is to test
369 whether deposition occurs within the suspension before withdrawal, and/or by a kind
370 of Langmuir-Blodgett effect during withdrawal. Doing so substrate is not driven
371 through water surface on which thin film of silicon oil may be present.

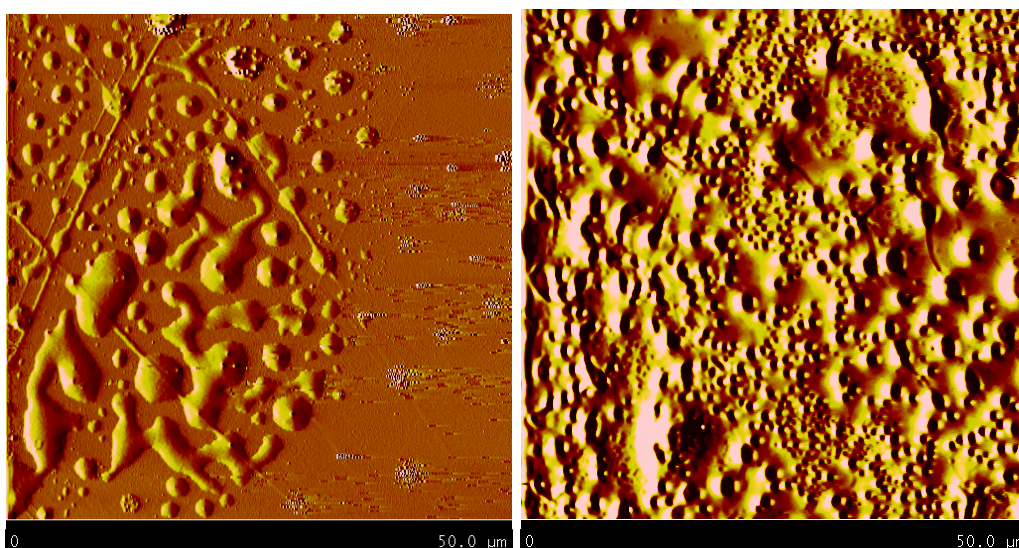
372

373 3. RESULTS FROM METHOD 1 – DROP ON SURFACE

374

375 Initial trials produced the AFM images shown in Figure 12. Here the undiluted
376 (50%) suspension was placed directly on a natural wafer. The left-hand image shows
377 the result of air drying, compared to vacuum drying on the right. The vacuum-dried
378 sample shows a thick, continuous film with pockmarks that we attribute to pockets of
379 water being evacuated from the film. The air dried sample shows much less coverage
380 and distinctive pools of oil, probably from coalescence of droplets across the surface
381 during drying.

382



383

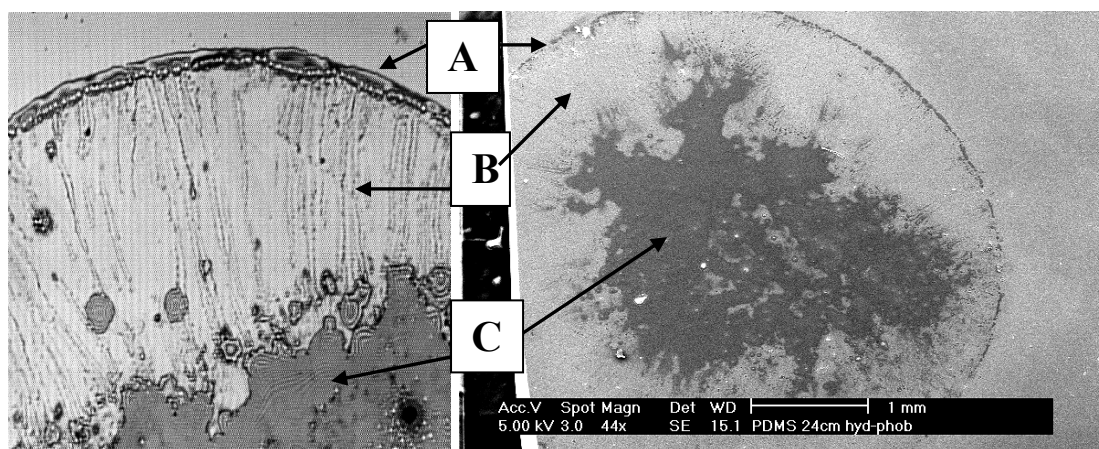
384

385 **Fig. 12.** AFM tapping mode images of PDMS on not treated (high contact angle) silicon wafers,
386 deposited from a drop of concentrated suspension that was subsequently dried. The images are 50 μm
387 frame, and show the result of deposition from an undiluted emulsion drop (50% v/v) followed by air
388 drying (left) and vacuum drying (right).

389

390 Subsequently it was found much easier to obtain consistent results by using
391 suspensions that had been diluted by 10^3 to 10^4 times. Using Method 1 gave a
392 suspension drop that did spread differently on the hydrophobic (high contact angle)
393 and hydrophilic (low contact angle) surfaces of mica and silicon wafer. When the
394 drop of dilute PDMS suspension was dried out on the hydrophobic silicon wafer, a
395 “coffee ring” pattern was observed (clearly seen in Figures 13) with deposited oil
396 concentrated around the edge of the original drop, and near the centre of the
397 circumference. Similar results were obtained on hydrophobised mica surface.

398



399

400

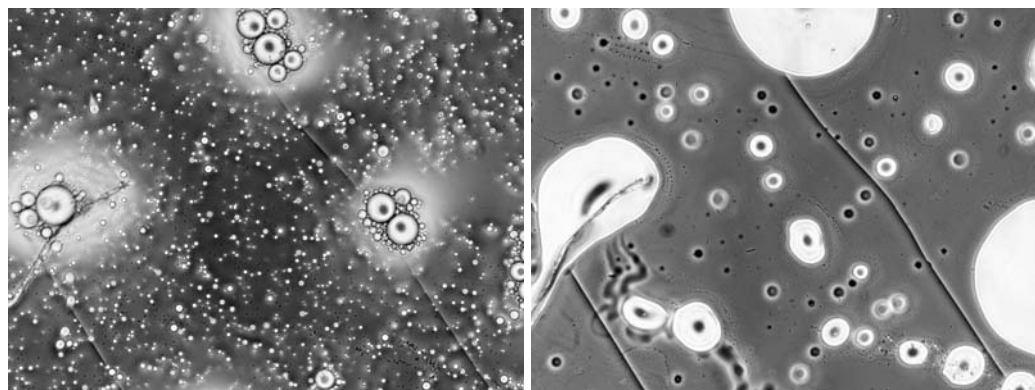
401 **Fig. 13.** Optical interference microscope image (left image) of substrate after diluted emulsion drops
402 were vacuum dried on the high contact angle wafer surface. The image, made in reflection using
403 monochromatic light, show constant-thickness interference fringes (Newton's rings) that can be used
404 to measure the height and profile of spread drops. The left-hand image shows the deposition from a
405 drop of emulsion diluted to about 0.025% PDMS. Regions mark respectively the coffee ring (A), a
406 sparse, stringy region(B) and the centre where oil is pooled (C). The right-hand image shows SEM
407 image of similar drop. The scale bars are 1 mm and this image was taken in secondary electron mode.

408

409 Both optical microscopy and SEM images show that there is concentration of oil
410 pools on former droplet circumference which developed in to “coffee ring” pattern
411 and in the central part of former droplet. In additional experiments droplets have been
412 observed during drying (Fig. 14). In micrographs obtained from optical microscopy
413 and shown in Fig. 14 can be deduced that because deposited diluted suspension
414 droplet has been anchored to the coffee ring circumference it did not change diameter
415 when drying. When drying it rather shallowing droplet to flatter pancakes like rather
416 than lenses like with significant curvature in central part of this droplet. During drying
417 small oil spheres in suspension were coalesce in many places within coffee ring
418 circumference. This coalescence did not occur in one place in the droplet centre but

419 randomly spread in island pattern within the circumference. Small oil droplets inside
420 suspension having buoyancy in natural way concentrate away from circumference of
421 the coffee ring pattern where water film is thinner and congregate rather near the
422 central part where thicker water film is still available. In the moment when water
423 evaporates all oil droplets aggregated within islands coalesced and turn into oil pools
424 in result as it is shown in Fig. 14.

425
426



427
428

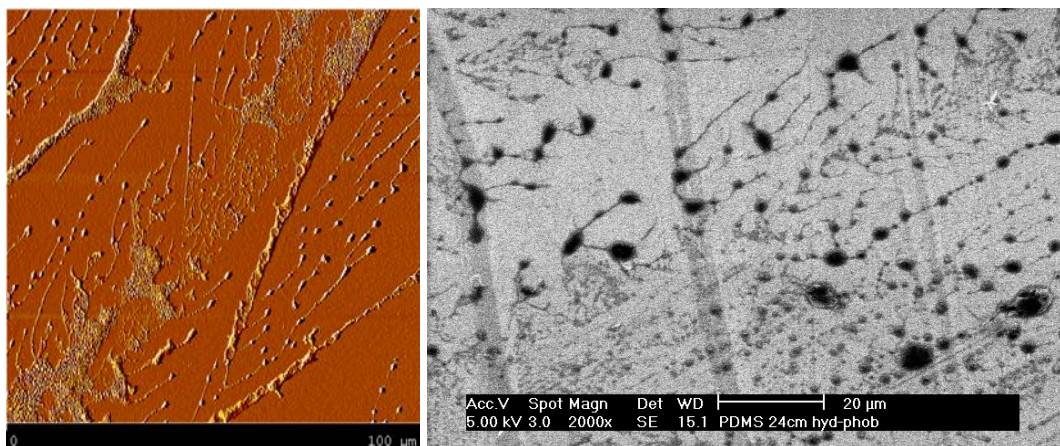
429 Fig. 14. Droplets of diluted PDMS suspension on hydrophobic substrate when drying show increase
430 larger oil spheres which coalesce in to larger oil pool.

431

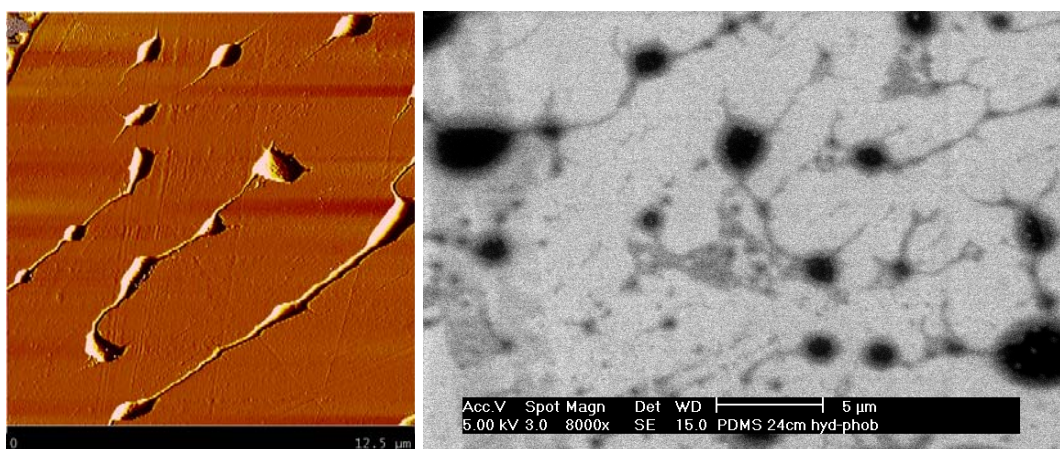
432 In Fig. 13 it is also visible that between coffee ring structure and the central oil
433 pools island is also very distinctive area where very small oil droplets were stretched
434 into radial oriented fibre like stringy patterns with obvious marks of stress being
435 experience during drying. These strings may be remnants of ruptured oil film which
436 covered whole suspension drop surface. This film could be formed even before
437 suspension droplet deposition onto the substrate.

438 Figure 15 shows AFM and SEM images of this stringy intermediate region at two
439 magnifications. It is clearly visible that oil was deposited from viscous fibre-like
440 stretched film rather than from spherical droplets. In the central region it appears that
441 a film of PDMS exists in the areas between the deposited droplets, but it is not clear
442 whether such a film exists in the areas between strings from the intermediate region.
443 Figure 15 shows an excellent correlation between SEM and the AFM images taken in
444 the stringy region in small and large magnification. Given their radial orientation, a
445 likely explanation for these strings is that they are formed as a result of the suspension
446 drop's surface PDMS film rupture during the final stages of drying. Figure 15 right
447 images shows similar features obtained with the SEM in secondary electron mode.

448



449
450



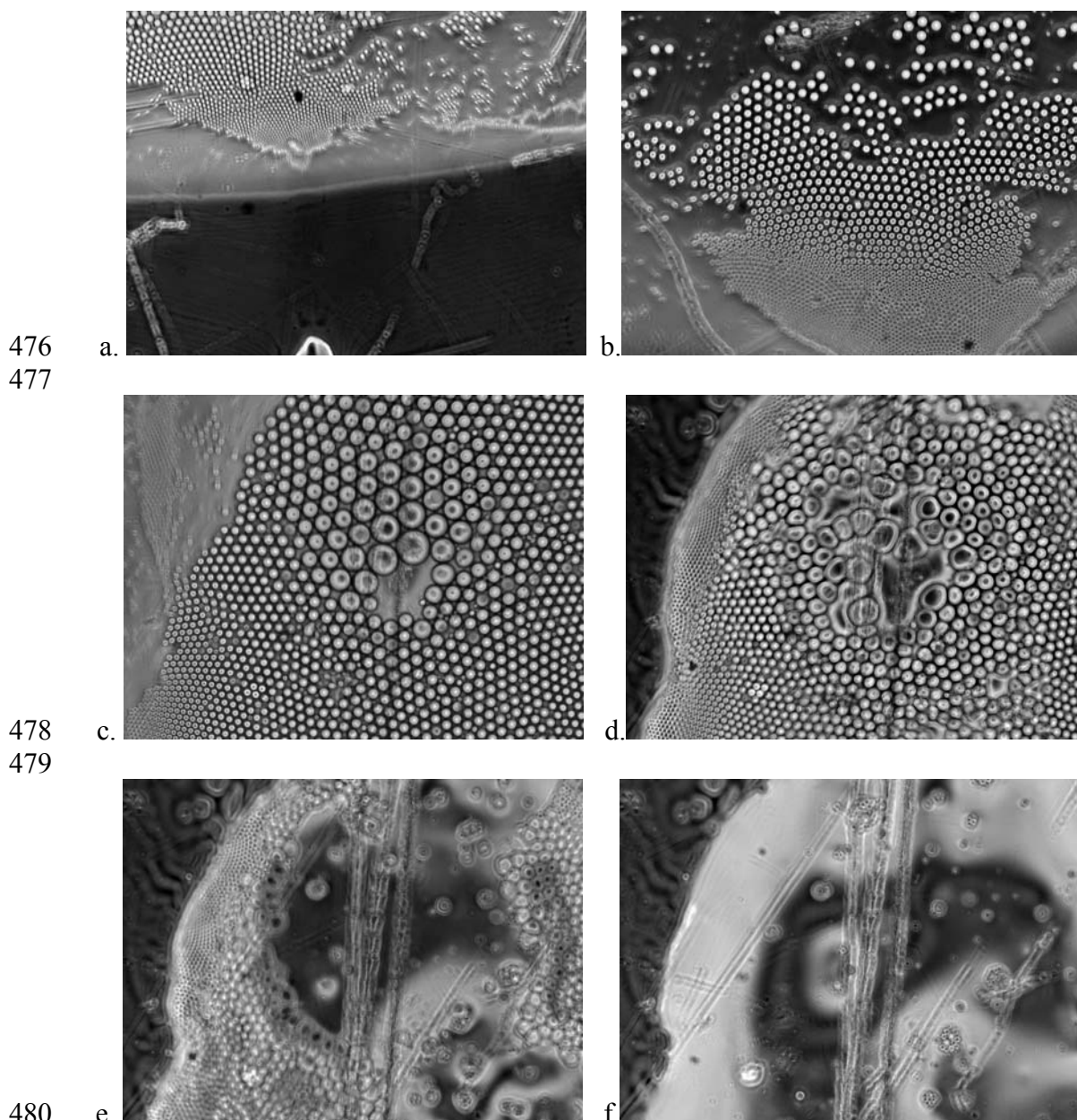
451
452
453
454
455
456
457

Fig. 15. Comparison between and AFM images (left) SEM images (right) of Region B, showing a clear similarity in the images taken by the different techniques. The scale bars of the secondary electron SEM images are 200 μm (upper right) and 5 μm (lower right), while the AFM images are of 100 μm (upper left) and 12.5 μm (lower left) squares.

458 In hydrophilic surfaces like on freshly cleaved mica and on plasma treated silicon
459 wafer the dynamic of drying the dilute PDMS suspension is different. There are not
460 coffee rings and because of it droplet is not anchored to the surface which allow the
461 shrink droplet diameter during drying. Fig 16 shows the dynamic of PDMS dilute
462 suspension drying. In this case, the macroscopic drop retracts smoothly as it dries,
463 with no pinning of its perimeter, no accumulation of PDMS drops there, and no
464 resultant coffee ring. Emulsion micro-spheres of PDMS accumulate at the surface of
465 the main drop, forming close-packed arrays with local hexagonal ordering giving a
466 “fly’s eye” appearance. The accumulation occurs at the apex of the drop, so it is
467 possible that gravity is having an effect (the buoyancy of PDMS pushing the spheres
468 to the highest part of the drop). This was investigated by placing the main drop
469 underneath as well as no top of the mica. It is also apparent that the PDMS spheres

470 near the apex of the main drop have a larger size, suggesting that coalescence is
471 occurring. After a fairly short time (a few minutes) the coalescence results in a larger
472 pool of PDMS forming at the apex – this is the phenomenon known as *creaming*.
473 Then, after drying, we observe that the coalesced pool of PDMS is deposited on the
474 substrate.

475



481 **Fig. 16.** Optical micrographs of deposition by drying in air of a dilute suspension of 10 μm PDMS
482 emulsion droplets on a hydrophilic surface (freshly-cleaved mica). The width of each image is 220 μm .
483 (a) Near the edge of the main drop which retracts smoothly over the surface as it dries. Emulsion
484 droplets of PDMS are pushed away from the drying edge toward the centre of the main drop. (b)
485 Larger droplets in the distribution are found towards the centre. (c) Large droplets appear at the apex
486 of the drop. It appears that some of the drops must have coalesced, since they are larger than the
487 original 10 μm emulsion droplet size. (d) The large drops at the apex coalesce to form bulk PDMS. (e)
488 A pool of bulk PDMS forms at the apex, and after drying, (f) it is deposited onto the substrate. In this

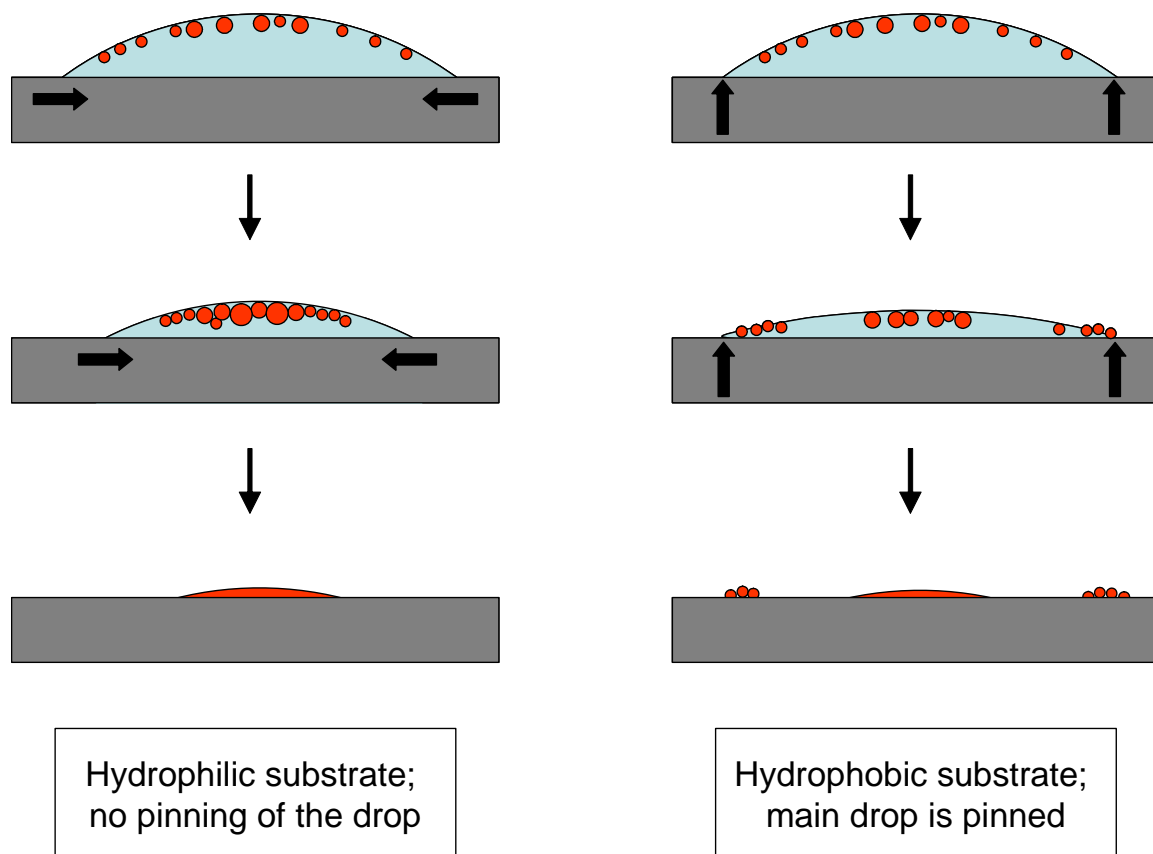
489 step, remaining emulsion droplets visible off-centre in (e) also coalesce. The whole process from (a) to
490 (f) occupies a few minutes. The rough vertical lines are scratches on the lower surface of the mica.
491 Focus was changed between images as the drop evaporated.

492
493 These observations help us to understand the textures that we have previously
494 observed with a coffee ring formed by forced drying of a suspension. In that case (on
495 a hydrophobic substrate) the perimeter of the main drop remains pinned during
496 drying, and some of the PDMS droplets after coalescence within the ring area are
497 attached to the perimeter and end up being deposited there to form the coffee ring.
498 However, other emulsion droplets probably behave in the same way as shown in
499 Figure 14, so that there are not many of them deposited near the coffee ring, still far
500 from the centre. A larger concentration – and probably a pool of bulk PDMS from
501 coalesced drops – is deposited onto the substrate near the centre of the coffee ring.
502 The two situations are sketched in Figure 17.

503 The difference in behaviour may or may not be due to the hydrophilicity
504 /hydrophobicity of the substrate. It appears (Figure 16a) that the more important
505 factor is whether or not the perimeter of the main drop can retract freely. Pinning may
506 be associated with surface lipophilicity more than the contact angle.

507

508



509

510 **Fig. 17** Schematic illustration of drying of a drop of suspension (blue) containing emulsion droplets of
 511 PDMS (red) with two types of behaviour that we have observed.

512 Statement that emulsion droplet retracts smoothly on the hydrophilic surface is
 513 however not entirely correct. Behind the retracting front some small morphological
 514 patterns are visible on some micrographs and they are similar to region B patterns
 515 from Fig. 13. This may suggest that all droplets may be covered by thin film of oil
 516 (probably monolayer) which may be not perfectly spread but rather net like covering
 517 the droplet surface. Fragments of this film may adhere to the substrate surface around
 518 retracted suspension droplet, but because of its minor quantity, it remains behind the
 519 retracting liquid droplet front as fragmented stringy patterns instead massive coffee
 520 ring patterns observed on hydrophobic substrate.

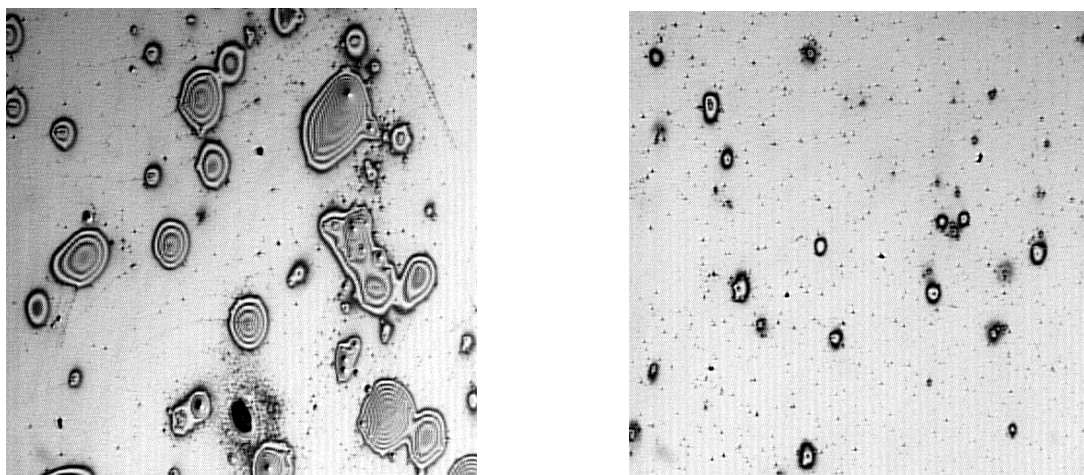
521 The nature of the PDMS deposited by forced drying (with or without the coffee
 522 ring caused by pinning of the perimeter) would therefore depend on the relative rate
 523 of drop drying compared to the rate of creaming. If the main drop dries quickly before
 524 drop coalescence or creaming progresses, the PDMS will be deposited as small
 525 emulsion droplets. However, if creaming is rapid, the PDMS will be deposited in the
 526 form of drops that are considerably larger than the original emulsion drops. It is also

527 possible that the droplet coalescence and creaming is forced by the increasing volume
528 fraction of PDMS in the suspension as the water evaporates, in which case it would be
529 an inevitable consequence of drying.

530 When method 1 is used with a wafer that has been made hydrophilic by plasma
531 treatment, the suspension drop spreads over most or the entire wafer, resulting in no
532 obvious coffee ring after drying, and a more uniform distribution of deposited drops
533 at a lower areal density. As seen in Figure 18, the density is lower when the original
534 drop has a lower concentration of emulsion. The larger droplets present on the surface
535 of the higher-concentration sample are presumably the result of droplet coalescence
536 when the surface density of emulsion droplets is higher.

537 Although it is not visible from the optical micrographs, there is a thin film covering
538 the wafer between the isolated drops. Ellipsometer measurements made in the regions
539 between the drops give a film thickness of 5.7 nm.

540



541

542

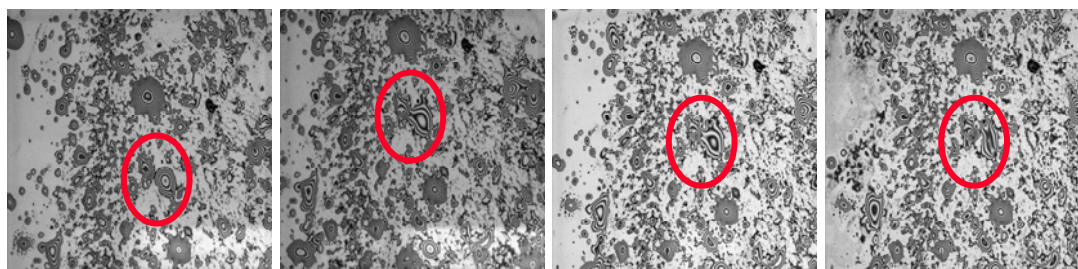
543 **Fig. 18.** Optical interference micrographs of 2 mm square regions showing PDMS emulsion droplets
544 deposited on a plasma-treated (hydrophilic) silicon wafer. In this case the suspension wets and spreads
545 over the whole wafer before being vacuum dried. The left-hand images show deposition from the
546 0.025% suspension and right-hand side from 0.006% suspension.

547

548 Images shown in Fig. 18 were taken with a low-resolution camera, and while they
549 are reasonably clear when viewing the electronic version of this document on a
550 computer screen, Moiré effects produce artefacts (regular patterns of lines) that tend
551 to obscure the images in the printed document. The second point is to note that
552 interference fringes are spaced at thickness intervals of $\lambda/2n$ (where n is the refractive
553 index of PDMS), which is about 240 nm. Hence the height of a droplet is about $(m/4)$
554 μm , where m is the number of fringes seen in the image of the droplet.

555 The following Figure (19) presents evidence that the PDMS droplets deposited on
556 a surface, either hydrophobic (top) or hydrophilic (bottom), continue to flatten and
557 spread over a long period of time, 3 days or more. The evidence is obtained by
558 observing a reduction in the number of interference fringes associated with each
559 identifiable droplet – think of the fringes as height contours on a map, at intervals of
560 240 nm.

561



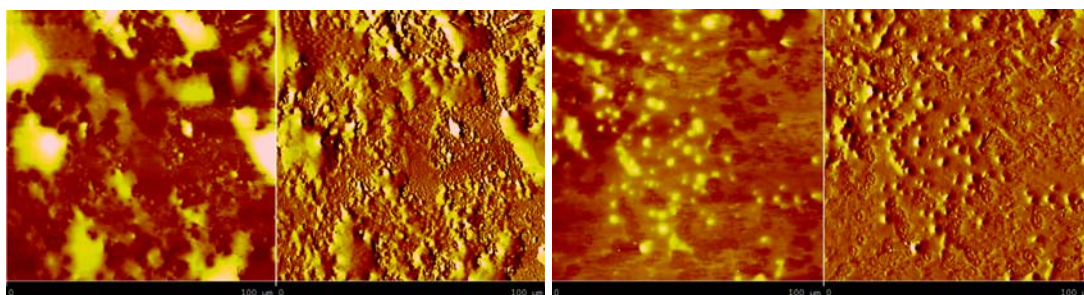
562

563 **Fig. 19** Optical interference images, each 0.85 mm on the long side, taken at (left to right) 10, 60, 150
564 and 3600 minutes after drying a 0.025% drop. The upper series shows PDMS on a normal
565 (hydrophobic) wafer and the lower set is for a plasma-treated (hydrophilic) one. Each fringe represents
566 a constant-thickness contour, with contour intervals of $\lambda/2n \approx 240$ nm. Hence the reduction with time
567 of the number of fringes in the same feature of the image shows progressive thinning of PDMS
568 droplets on the surface. Locating the same features in the lower series is not so evident except in the
569 central two images, but the thickness reduction is clear even from these two.

570

571 The AFM images in Fig. 20 show continuous (though not smooth) films on both
572 the hydrophobic and hydrophilic surfaces 60 hours after deposition.

573



574

575

576 **Fig. 20.** AFM images of the same samples as in Fig. 21 after 3600 minutes (60 hours). The left-hand
577 pair is for the hydrophobic wafer and the right-hand pair is for the hydrophilic one. An uneven but
578 apparently continuous film is evident on both surfaces.

579

580

581 **4. RESULTS FROM METHOD 2 – AFTER IMMERSION IN EMULSION**

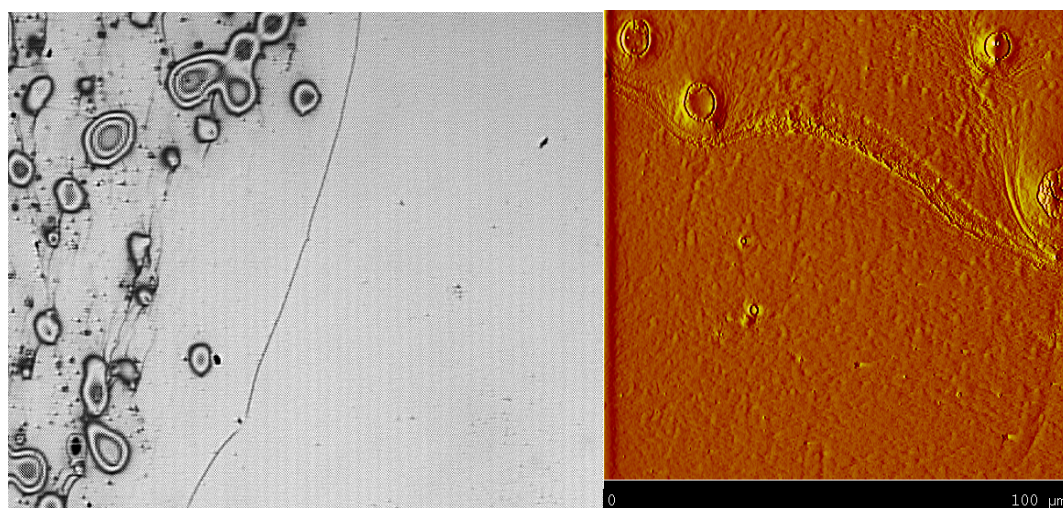
582

583 Optical interference micrographs of a plasma-treated silicon wafer that has been
584 immersed in the suspension then withdrawn and vacuum dried are shown in Fig. 21.

585 The wafer is withdrawn more or less vertically, and since it is hydrophilic a water

586 film coats it, with an excess of water hanging from the bottom edge. When the wafer
587 is placed horizontally prior to drying, this drop spreads back over the wafer, forming a
588 thick film over part of the surface while the remainder is covered by a thinner film.
589 The left-hand image in Fig. 21 shows the PDMS deposited in the thick-film region
590 (on the left side of the image and the thin-film region is on right side of the thin
591 dividing line. The AFM image show also the dividing line and the thick (upper part of
592 this image) and thin (lower part of this image) film regions. There appears to be a
593 continuous film of PDMS with a scaly appearance in both regions, but it looks thicker
594 on the top of this image. This is confirmed by ellipsometry measurements (made
595 between drops), which give thicknesses of 11.7 nm and 4.1 nm for the thick and thin
596 film regions respectively.

597



598
599

600 **Fig. 21.** Optical interference (2 mm square) and AFM images (100 μm square) of PDMS deposited on
601 hydrophilic silicon wafer by immersion in and withdrawal from a diluted emulsion, then vacuum
602 drying. The left-hand images show deposition from a thick film and the right-hand side from a thin
603 film region (see text).

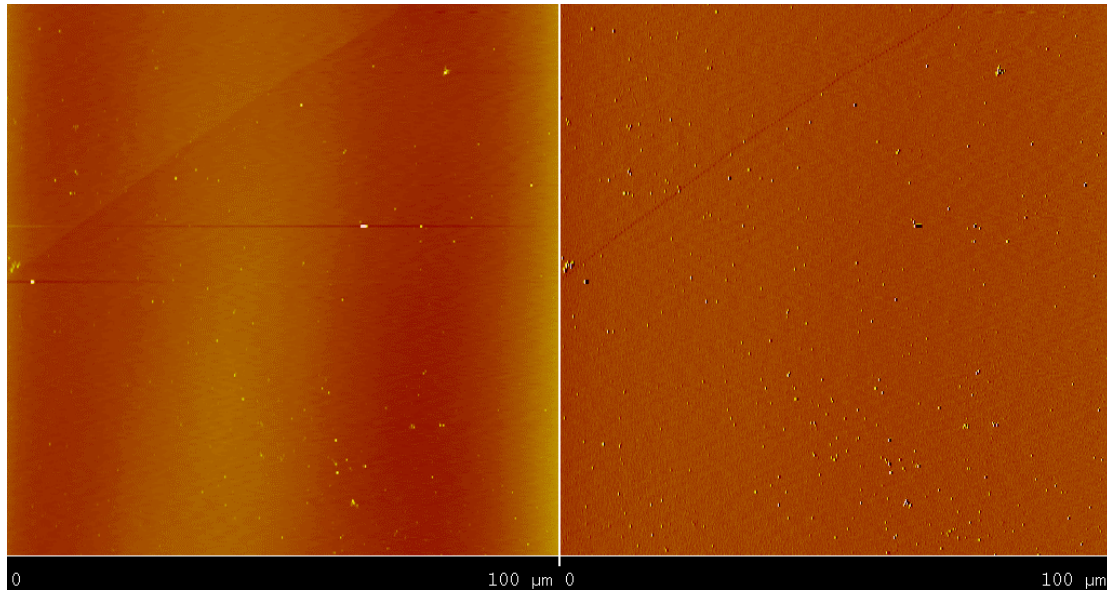
604

605

606 A much reduced amount of PDMS is deposited if the suspension in which a wafer
607 is immersed is greatly diluted before the wafer is withdrawn and dried. This supports
608 the evidence from Method 2b (Fig. 19) and demonstrates that little or no deposition
609 occurs while the wafer is immersed in the suspension. The small amount that does
610 adsorb is probably present in the highly diluted suspension that is entrained with the
611 wafer on withdrawal, and deposited during drying.

612

613



614
615
616
617
618
619

Fig. 22 AFM images (100 μm square) showing two regions of the Method 3 sample. Droplet deposition is sparse.

620 The AFM images in Fig 22, while unable to show large areas of the surface,
621 indicate that deposited droplets are few and far between. Ellipsometry measurements
622 also suggest that there is little or no film present between the drops, although the
623 result for film thickness could be between 0 and 2.5 nm depending on the assumptions
624 made about the optical properties of the substrate and in particular, whether the
625 ubiquitous thin oxide layer on the silicon wafer is removed by the plasma treatment.

626 The droplets do not appear to increase in their diameter on the surface, and they
627 are too far apart to coalesce with each other. These facts suggest that the droplet
628 volumes decrease as they flatten, and (apart from the unlikely occurrence of
629 evaporation) the only place for the PDMS to go is into a thin film between the visible
630 drops.

631

632 **4. SUMMARY**

633

634 In this paper a brief review has been presented of previous observations of
635 spreading of PDMS drops on silicon wafers. The literature includes a number of
636 experiments which have used ellipsometry techniques to observe the presence and
637 measure the dimensions of a precursor film spreading ahead of, and faster than, the
638 main drop.

639 We have presented our own measurements using an imaging ellipsometer, which
640 also clearly shows the presence of a precursor film. The diffusion constant of this
641 film, measured with a 60 000 cS PDMS sample spreading on a hydrophilic silicon
642 wafer, is $D_f = 1.4 \times 10^{-11} \text{ m}^2/\text{s}$.

643 Series of investigations has been also conducted on the morphological patterns of
644 PDMS diluted emulsion spreading on hydrophobic and hydrophilic surface of silicon
645 wafer and mica. A qualitative rather than quantitative investigation of droplet size,
646 shape, coverage and spreading were resulted from this study. It was intended mainly
647 to show what is possible with the different observation techniques for future
648 investigations of deposition of PDMS emulsion droplets.

649 Scanning Electron Microscopy can produce good images over a wide range of
650 magnifications, correlating well with optical micrographs at low magnification and
651 AFM images at high magnification. However, since it does not add significantly to
652 what can be observed with optical microscopy and AFM and it is more tedious to use,
653 SEM will probably not be used for the further studies.

654 AFM and optical interference microscopy can both give good measurements of
655 drop shapes (heights and diameters). Furthermore, they can both be used to monitor
656 changes with time of the deposited drop dimensions. Optical microscopy would be
657 more convenient for following changes that occur over a long time (more than several
658 hours, say) but can only be used for larger drops, whose spread diameter is $\sim 10 \mu\text{m}$ or
659 more.

660 None of the microscopies can give accurate measurements of the thickness of
661 nanometric films that are often found around or between droplets deposited on
662 surfaces. For this, ellipsometry is ideal, and the imaging ellipsometer is particularly
663 useful because the measurements can be made in the regions between droplets only,
664 as long as the latter are reasonably spaced.

665 The qualitative observations made include the fact that droplets from this PDMS
666 emulsion ($10 \mu\text{m}$ droplets stabilized by a nonionic surfactant) are only deposited by
667 forced drying of the suspension.

668 A “coffee ring” effect is observed on hydrophobic wafers, on which the aqueous
669 suspension drop beads up and emulsion droplets concentrate at the perimeter of the
670 drop as it dries, and are deposited there. However, there is evidence suggesting that in
671 the final stages of drying the main drop does not remain pinned at its perimeter, but

672 ruptures, dragging emulsion drops with it and depositing the majority of the PDMS
673 near the centre and leaving radially oriented stringy region in between.

674 Deposition by forced drying occurs on both hydrophobic and hydrophilic wafers,
675 with the main difference being that in the latter case there is no coffee ring effect
676 because the suspension spreads is not pinned in to the wafer surface and retracts is
677 more uniform and forms in effect central oil pool from PDMS micro-spheres
678 coalescence.

679 Regardless of their size, density and method of deposition, droplets on both types
680 of wafer (hydrophilic and hydrophobic) flatten out over a period of many hours, up to
681 3 days. During this process neighbouring droplets may coalesce, but there is strong
682 evidence that some of the PDMS from the droplets migrates into a thin, continuous
683 film that covers the surface in between droplets.

684 The thin film appears to be ubiquitous if there has been any deposition of PDMS.
685 However, this statement needs further verification. One question is whether the film
686 forms immediately after forced drying, or whether in some or all cases it only forms
687 by spreading from isolated droplets as they slowly flatten out.

688

689

690 *Acknowledgements*- The author would like to acknowledge Prof. Roger Horn from Ian
691 Wark Research Institute, University of South Australia under whom inspiration,
692 supervision and leadership this work was conducted.

693

694

695

696 **REFERENCES**

697

698 [1] A. M. Cazabat, *Contemp. Phys.* 28(4), (1987) 347-364

699 [2] B.V. Derjaguin, N.V. Churaev, *Wetting Films* (nauka, Moscow, 1984) in
700 Russian.

701 [3] P.G. de Gennes, *Rev. Mod. Phys.* 57 (1985) 827

702 [4] J. Daillant, J.J. Benattar, L. Bosio, L. Leger, *Europhys. Lett.* 6(5), (1988) 431-
703 436

704 [5] L. Leger, M. Erman, A.M. Guinet, D. Ausserre, G. Strazielle, *Phys. Rev. Lett.*
705 60, (1988) 2390-2393

706 [6] L. Leger, M. Erman, A.M. Guinet-Picart, D. Ausserre, G. Strazielle, J.J.
707 Benattar, F. Rieutord, J. Daillant, L. Bosio, *Revue Phys. Appl.* 23, (1988) 1047-
708 1054

709 [7] D. Beaglehole, *J. Phys. Chem.* 93, (1989) 893-899

710 [8] F. Heslot, N. Fraysse, A.M. Cazabat, *Nature*, 338, (1989)640-642

711 [9] F. Heslot, A.M. Cazabat, P. Levinson, N. Fraysse, *Physical Review Letters.*
712 65(5), (1990) 599-601

713 [10] R.G. Horn, J.N. Israelachvili, *Macromolecules*, 21, (1988) 2836-2841

714 [11] E.Perez, E. Schaffer, U. Steiner, *J. Colloid Int. Sci.* 234, (2001) 178-193

715 [12] P.G. de Gennes, *Rev. mod. Phys.*, 57, (1985) 827

716 [13] D. Ausserre, A.M. Picard, L. Leger, *Phys. Rev. Lett.*, 57 (1986) 2671

717 [14] D. Beaglehole, *Physica B*, 100, (1980) 163-175

718 [15] P.G. de Gennes, F. Brochard-Wyart, D. Quere, *Capillarity and Wetting*
719 *Phenomena*. Springer. (2004) 291

720 [16] R. Fondecave, A. Buguin, F. Brochard, Laboratoire de physico-chimie Curie,
721 Institut Curie, Paris, Fr. *Comptes Rendus de l'Academie des Sciences, Serie*
722 *Iib: Mecanique, Physique, Astronomie* (1999), 327(4), 407-414.

723

724

725 **Figure captions**

726 Fig. 1 Thickness maps surrounding a PDMS drop deposited on the plasma
727 cleaned silicon wafer.

728

729 Fig. 2 SEM micrograph of silicon oil drop at the beginning of the experiment and
730 after one hour. Bright ring of precursor film evolve.

731 Fig. 3 Increase of drop radius and precursor film width with time, estimated from
732 the images in Figs. 1 & 2. The upper plot has time on a linear scale; the lower one
733 compares precursor film width to \sqrt{t} .

734 Fig. 4 Increase of drop radius and precursor film width with time, estimated from
735 the images in Fig. 1. The upper plot has time on a linear scale; the lower one
736 compares precursor film width to \sqrt{t} .

737 Fig. 5 AFM 3-dimensional image of macroscopic droplet with possible precursor
738 film advancing around its perimeter.

739 Fig. 6 SEM (a) and optical microscopy observations (b – white light and c-
740 monochromatic light) of merging oil droplets which differ in size.

741

742 Fig. 7 AFM 3-dimensional images showing the gradual coalescence of a small
743 silicone drop with a large one. Image b was taken 100 minute after image a have been
744 recorded. The area is $100 \mu\text{m} \times 100 \mu\text{m}$. © The time evolution of shape parameters of
745 the small drop taken from Figure 7c.

746 Fig. 8 Optical micrographs of a silicone drop spreading on a silicon wafer in air.
747 Shape analysis of the optical images from, showing the spreading and flattening of
748 the drop. Note the large decrease in contact angle from 70° to less than 10° over 200
749 minutes for this 60,000 cS silicone on silicon in air.

750 Fig. 9 Optical images of a 0.7 mm diameter silicone drop on a silicon wafer
751 under water, showing that in this environment it does not spread, over a time frame
752 similar to that of Fig. 8.

753 Fig. 10. Optical images of a water drop pressed onto a silicon wafer that was
754 previous covered with a thin (A) or thick (B) layer of silicone oil. The syringe
755 diameter is 1 mm. In (B) a faint, roughly horizontal, line can be seen about 1/3 of the
756 way up the drop on the left-hand side. We think this is a silicone/water/air three-
757 phase line as illustrated schematically in (C), where θ_1 is the contact angle of water
758 on silicon underneath silicone oil, and θ_2 is the contact angle of silicone oil on water
759 in air.

760 Fig. 11. Illustrating the three methods to test deposition of emulsion drops onto a
761 flat solid substrate. In Method 1 (top) a drop of emulsion is placed on a horizontal
762 substrate and then dried. In Method 2a (middle) the substrate is immersed in the
763 emulsion for several minutes, withdrawn and then dried. A variation (2b) is to rinse
764 the suspension from the wafer after withdrawal and before drying. Method 3 (bottom)
765 is similar to the second, except that substrate is immersed in pure water and
766 subsequently emulsion is produce by addition of concentrated emulsion droplets,
767 latter is diluted by copious amounts of water before withdrawing the substrate and
768 drying it.

769 Fig. 12. AFM tapping mode images of PDMS on not treated (high contact angle)
770 silicon wafers, deposited from a drop of concentrated suspension that was
771 subsequently dried. The images are $50 \mu\text{m}$ frame, and show the result of deposition
772 from an undiluted emulsion drop (50% v/v) followed by air drying (left) and vacuum
773 drying (right).

774 Fig. 13. Optical interference microscope image (left image) of substrate after
775 diluted emulsion drops were vacuum dried on the high contact angle wafer surface.
776 The image, made in reflection using monochromatic light, show constant-thickness
777 interference fringes (Newton's rings) that can be used to measure the height and
778 profile of spread drops. The left-hand image shows the deposition from a drop of
779 emulsion diluted to about 0.025% PDMS. Regions mark respectively the coffee ring
780 (A), a sparse, stringy region(B) and the centre where oil is pooled (C). The right-hand
781 image shows SEM image of similar drop. The scale bars are 1 mm and this image
782 was taken in secondary electron mode.

783 Fig. 14. Droplets of diluted PDMS suspension on hydrophobic substrate when
784 draying show increase larger oil spheres which coalesce in to larger oil pool.

785 Fig. 15. Comparison between and AFM images (left) SEM images (right) of
786 Region B, showing a clear similarity in the images taken by the different techniques.
787 The scale bars of the secondary electron SEM images are 200 μm (upper right) and 5
788 μm (lower right), while the AFM images are of 100 μm (upper left) and 12.5 μm
789 (lower left) squares.

790 Fig. 16. Optical micrographs of deposition by drying in air of a dilute suspension
791 of 10 μm PDMS emulsion droplets on a hydrophilic surface (freshly-cleaved mica).
792 The width of each image is 220 μm . (a) Near the edge of the main drop which retracts
793 smoothly over the surface as it dries. Emulsion droplets of PDMS are pushed away
794 from the drying edge toward the centre of the main drop. (b) Larger droplets in the
795 distribution are found towards the centre. (c) Large droplets appear at the apex of the
796 drop. It appears that some of the drops must have coalesced, since they are larger than
797 the original 10 μm emulsion droplet size. (d) The large drops at the apex coalesce to
798 form bulk PDMS. (e) A pool of bulk PDMS forms at the apex, and after drying, (f) it
799 is deposited onto the substrate. In this step, remaining emulsion droplets visible off-
800 centre in (e) also coalesce. The whole process from (a) to (f) occupies a few minutes.
801 The rough vertical lines are scratches on the lower surface of the mica. Focus was
802 changed between images as the drop evaporated.

803 Fig. 17 Schematic illustration of drying of a drop of suspension (blue) containing
804 emulsion droplets of PDMS (red) with two types of behaviour that we have observed.

805 Fig. 18. Optical interference micrographs of 2 mm square regions showing
806 PDMS emulsion droplets deposited on a plasma-treated (hydrophilic) silicon wafer.
807 In this case the suspension wets and spreads over the whole wafer before being
808 vacuum dried. The left-hand images shows deposition from the 0.025% suspension
809 and right-hand side from 0.006% suspension.

810 Fig. 19 Optical interference images, each 0.85 mm on the long side, taken at (left
811 to right) 10, 60, 150 and 3600 minutes after drying a 0.025% drop. The upper series
812 shows PDMS on a normal (hydrophobic) wafer and the lower set is for a plasma-
813 treated (hydrophilic) one. Each fringe represents a constant-thickness contour, with
814 contour intervals of $\lambda/2n \approx 240$ nm. Hence the reduction with time of the number of
815 fringes in the same feature of the image shows progressive thinning of PDMS
816 droplets on the surface. Locating the same features in the lower series is not so
817 evident except in the central two images, but the thickness reduction is clear even
818 from these two.

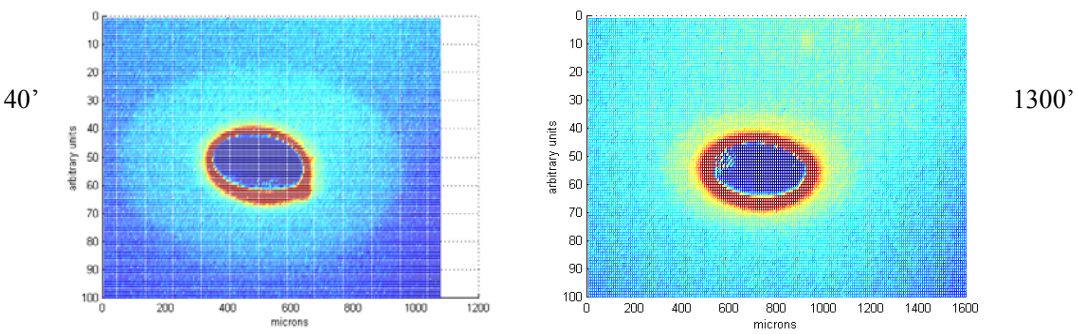
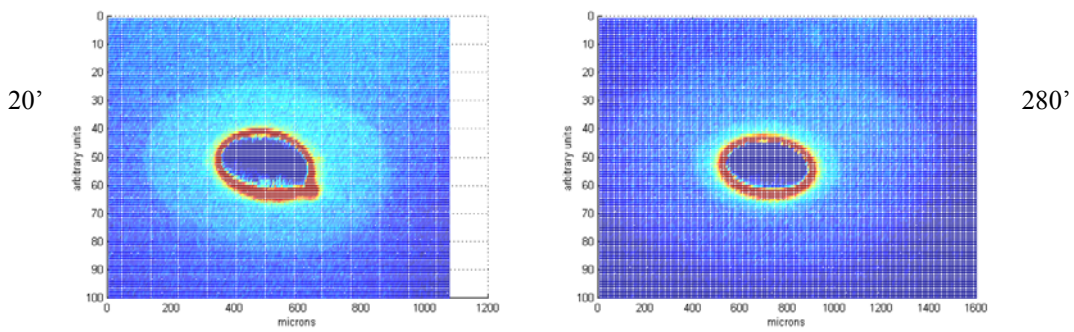
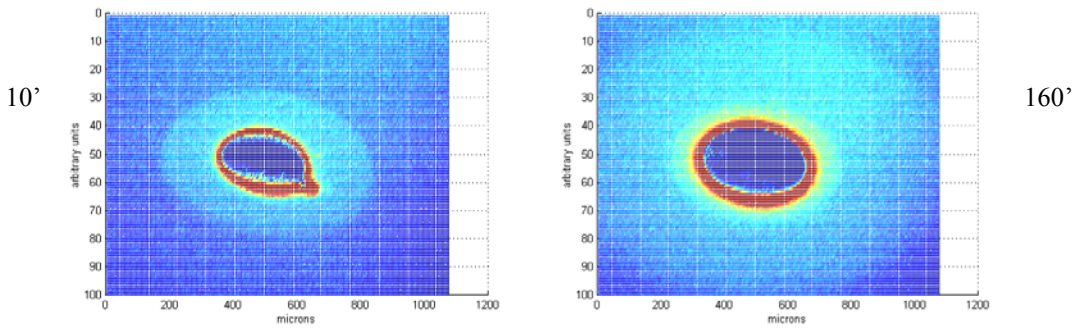
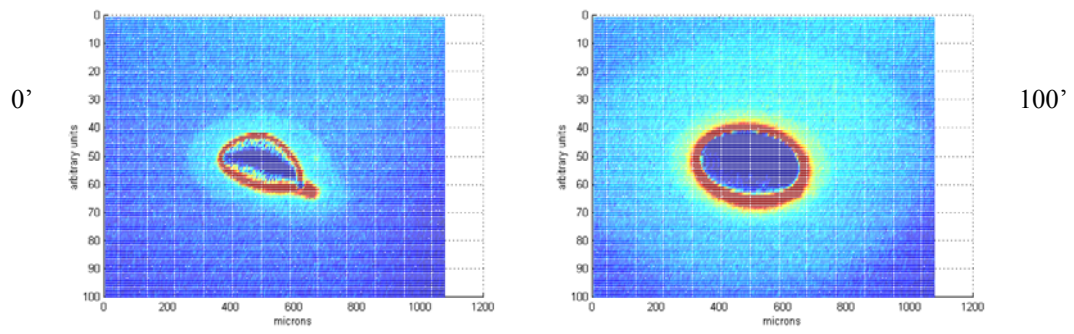
819 Fig. 20. AFM images of the same samples as in Fig. 21 after 3600 minutes (60
820 hours). The left-hand pair is for the hydrophobic wafer and the right-hand pair is for
821 the hydrophilic one. An uneven but apparently continuous film is evident on both
822 surfaces.

823 Fig. 21. Optical interference (2 mm square) and AFM images (100 μm square) of
824 PDMS deposited on a hydrophilic silicon wafer by immersion in and withdrawal
825 from a diluted emulsion, then vacuum drying. The left-hand images show deposition
826 from a thick film and the right-hand side from a thin film region (see text).

827 Fig. 22 AFM images (100 μm square) showing two regions of the Method 3
828 sample. Droplet deposition is sparse.

829
830
831
832

833
834



838

839

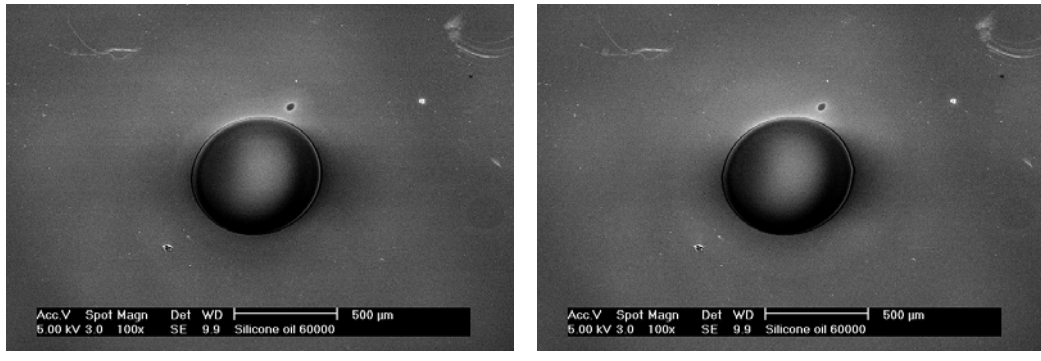
Fig. 1. Thickness maps surrounding a PDMS drop deposited on the plasma cleaned silicon wafer.

840

841

842

843



844

845

846

847 **Fig. 2. SEM micrograph of silicon oil drop at the beginning of the experiment**

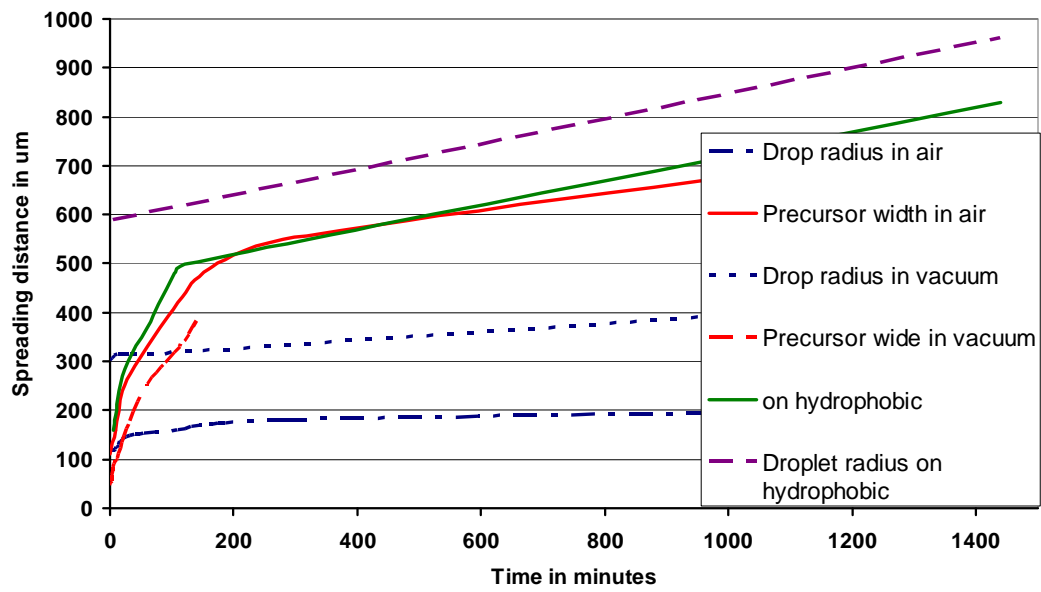
848 **and after one hour. Bright ring of precursor film evolve.**

849

850

851

852

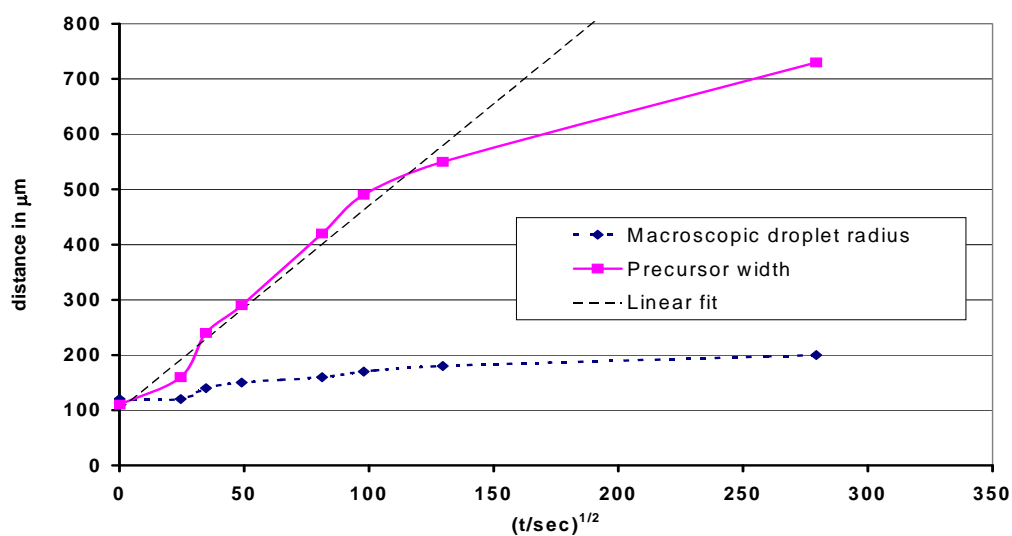


853
854

855 **Fig. 3. Increase of drop radius and precursor film width with time, estimated**
856 **from the images in Figs. 1 & 2. The upper plot has time on a linear**
857 **scale; the lower one compares precursor film width to \sqrt{t} .**

858

859



860

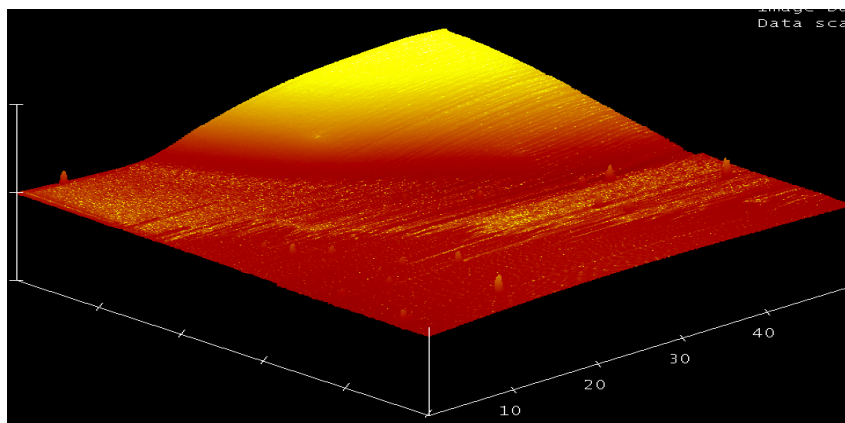
861

862 **Fig. 4. Increase of drop radius and precursor film width with time, estimated**
863 **from the images in Fig. 1. The upper plot has time on a linear scale; the**
864 **lower one compares precursor film width to \sqrt{t} .**

865

866

867



868

869

870

871 **Fig. 5. AFM 3-dimensional image of macroscopic droplet with possible**

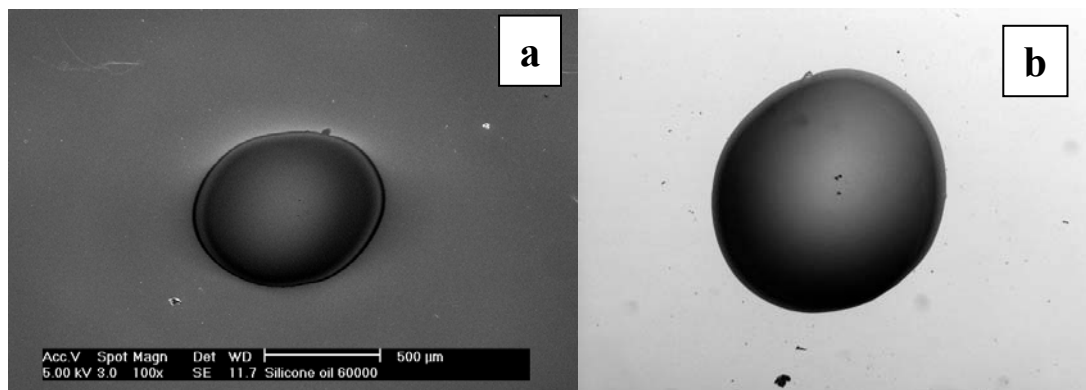
872 **precursor film advancing around its perimeter.**

873

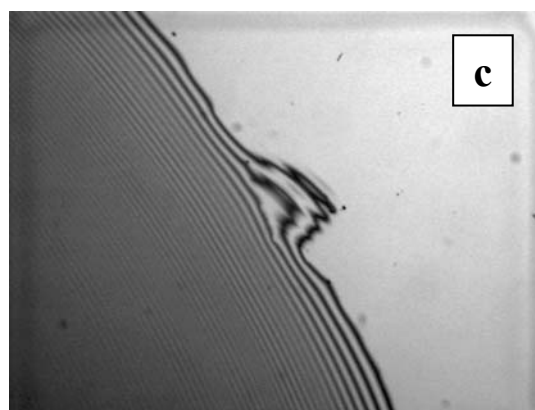
874

875

876



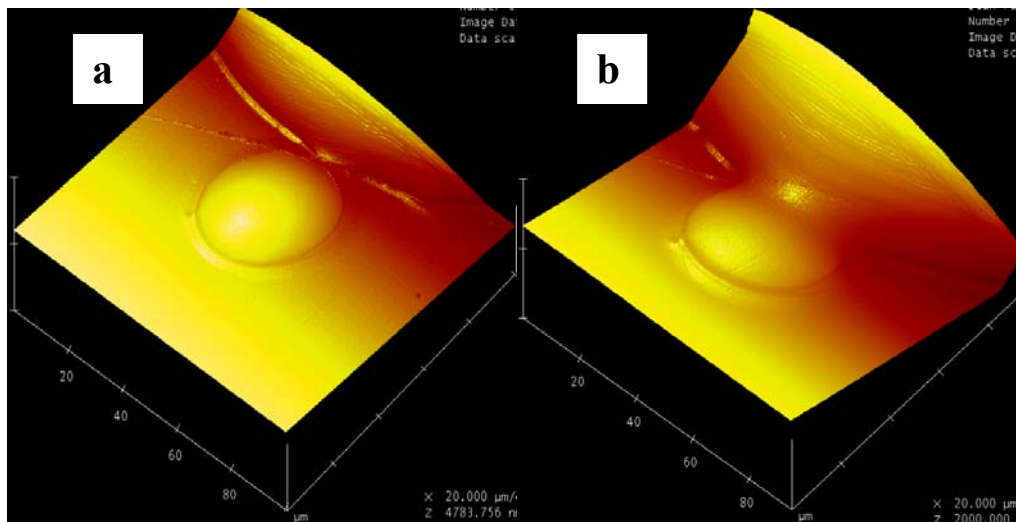
877
878



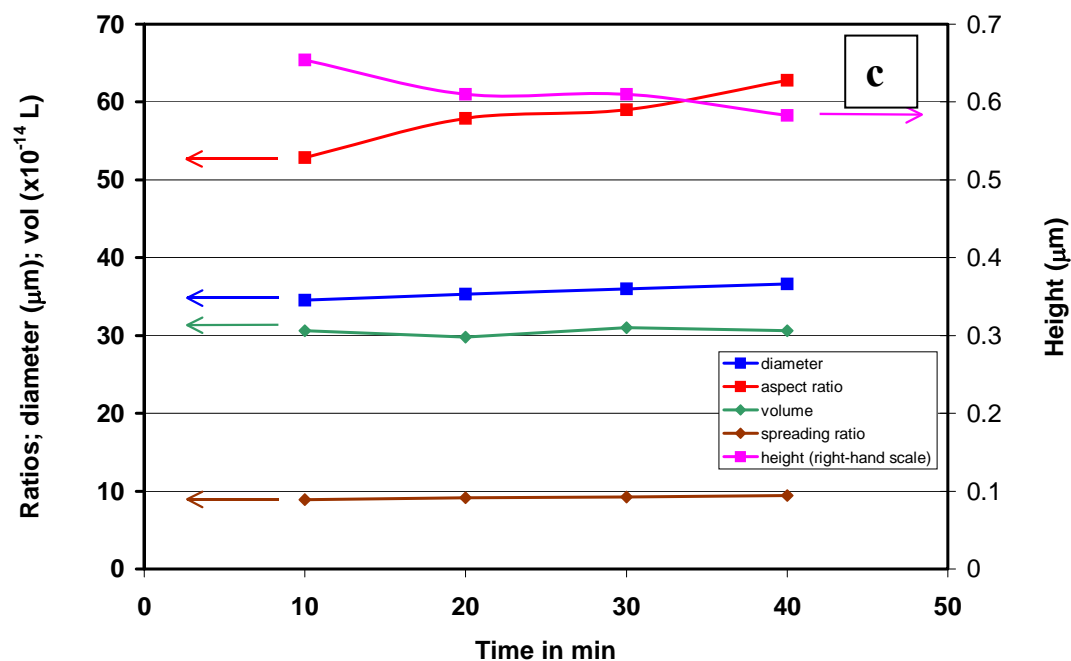
879
880
881
882
883
884
885

**Fig. 6. SEM (a) and optical microscopy observations (b – white light and c-
monochromatic light) of merging oil droplets which differ in size.**

886

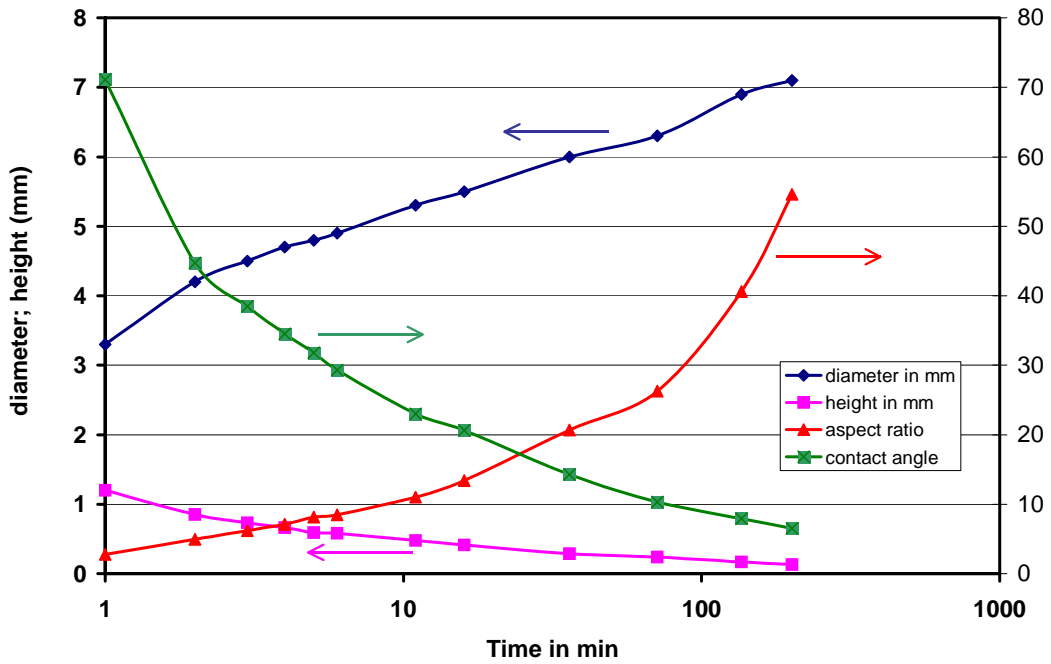


887
888

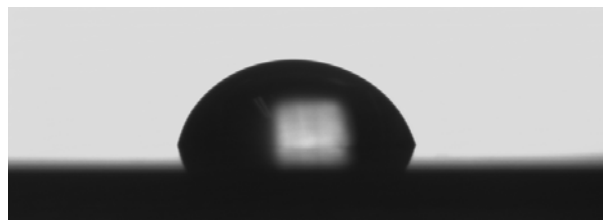


889
890
891
892
893
894
895
896
897

Fig. 7. AFM 3-dimensional images showing the gradual coalescence of a small silicone drop with a large one. Image b was taken 100 minute after image a have been recorded. The area is 100 μm × 100 μm. © The time evolution of shape parameters of the small drop taken from Figure 7c.



898



1 min

899

900

901



36 min

902

903

904



201 min

905

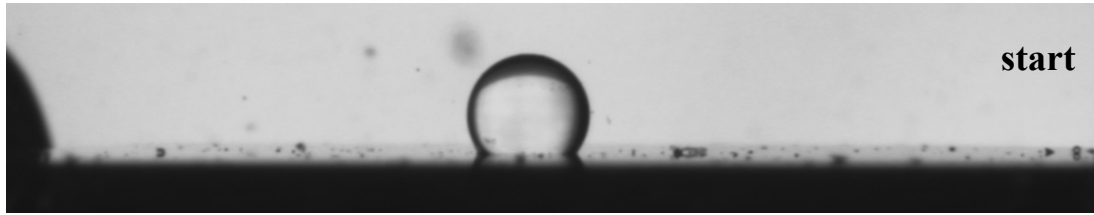
906

907

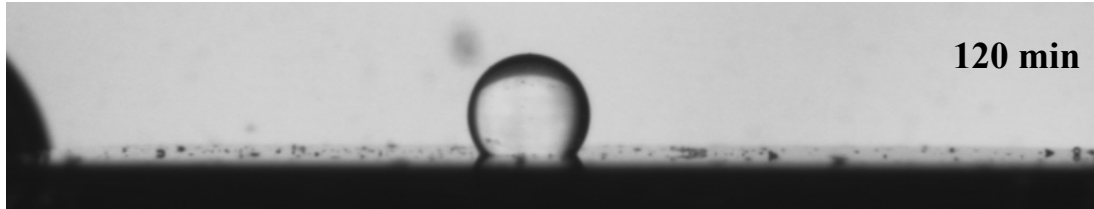
908

909 **Fig. 8** Optical micrographs of a silicone drop spreading on a silicon wafer in
 910 air. Shape analysis of the optical images from, showing the spreading and flattening of the drop. Note the large decrease in contact angle from
 911 70° to less than 10° over 200 minutes for this 60,000 cS silicone on silicon
 912 in air.
 913
 914

915



916
917

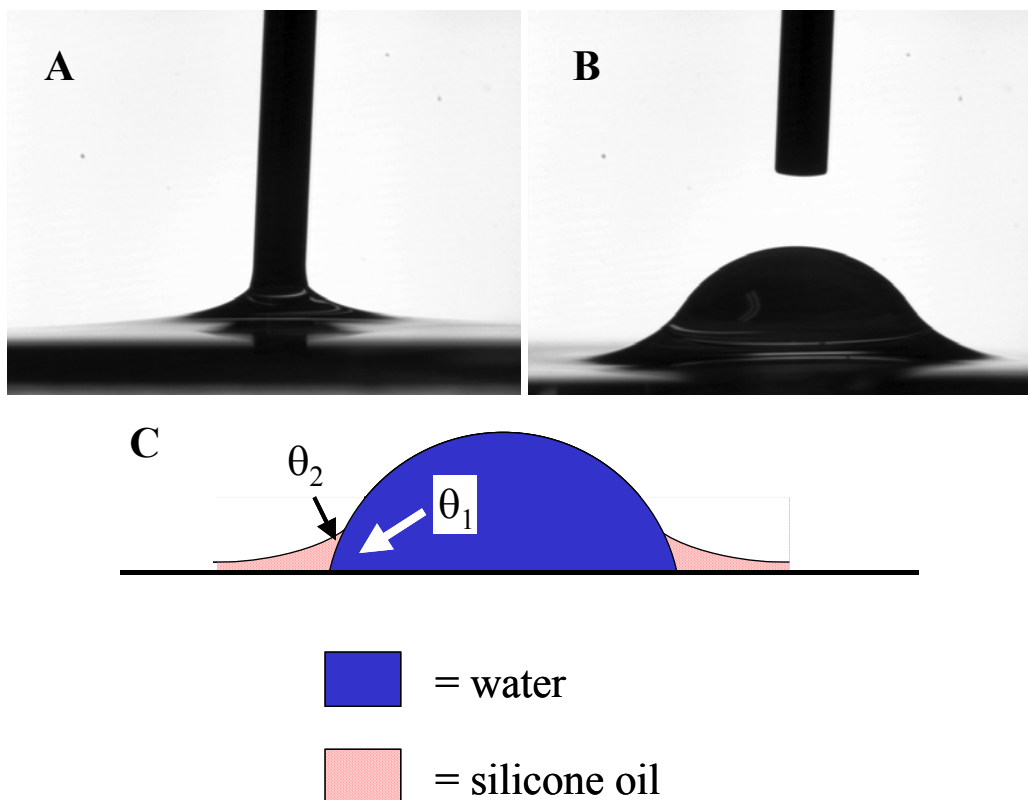


918
919
920
921
922
923
924
925

Fig. 9 Optical images of a 0.7 mm diameter silicone drop on a silicon wafer under water, showing that in this environment it does not spread, over a time frame similar to that of Fig. 8.

926

927



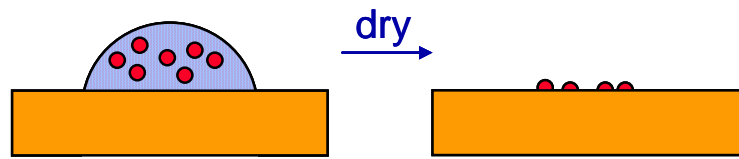
928
929

930
931
932

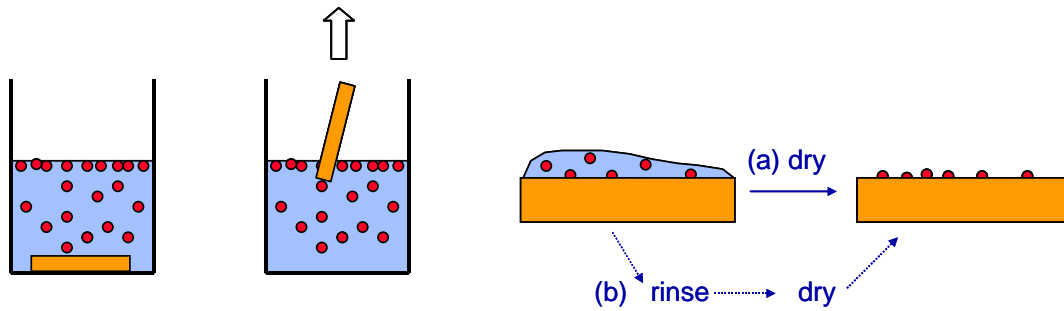
933 **Fig. 10.** Optical images of a water drop pressed onto a silicon wafer that was
934 previous covered with a thin (A) or thick (B) layer of silicone oil. The
935 syringe diameter is 1 mm. In (B) a faint, roughly horizontal, line can be
936 seen about 1/3 of the way up the drop on the left-hand side. We think
937 this is a silicone/water/air three-phase line as illustrated schematically
938 in (C), where θ_1 is the contact angle of water on silicon underneath
939 silicone oil, and θ_2 is the contact angle of silicone oil on water in air.

940
941
942

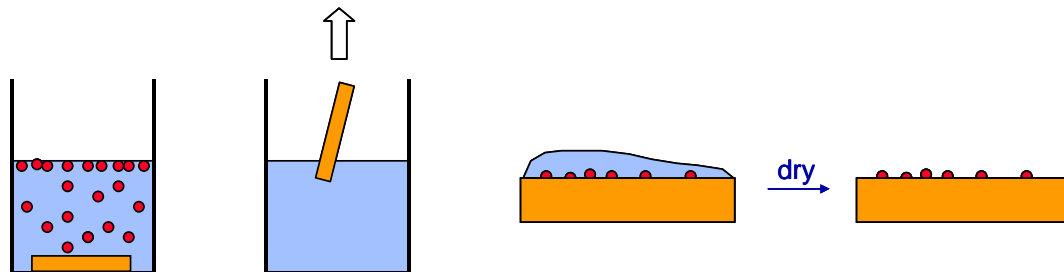
943



944



945



946

947

948

949

950

951

952

953

954

955

956

957

958

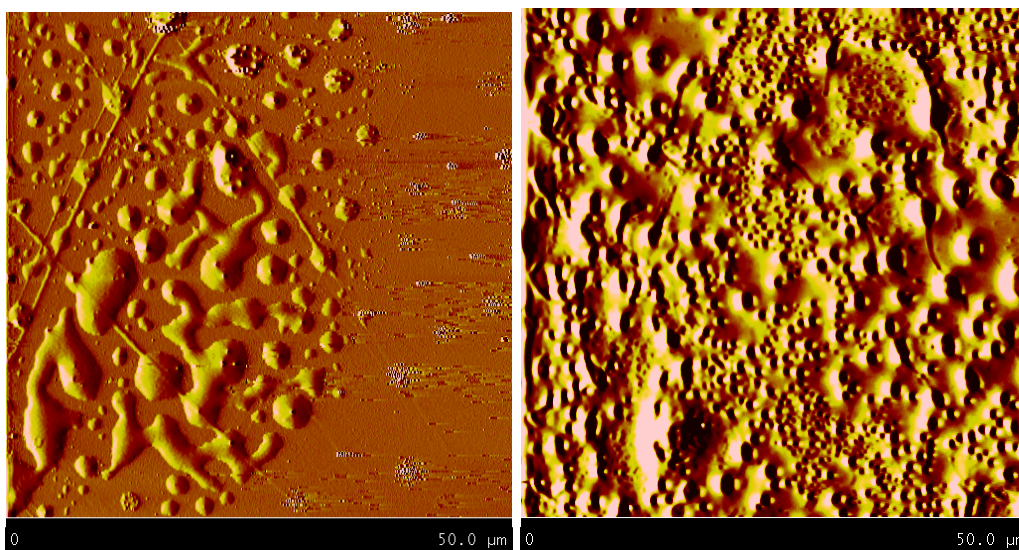
959

960

961

962

Fig. 11. Illustrating the three methods to test deposition of emulsion drops onto a flat solid substrate. In Method 1 (top) a drop of emulsion is placed on a horizontal substrate and then dried. In Method 2a (middle) the substrate is immersed in the emulsion for several minutes, withdrawn and then dried. A variation (2b) is to rinse the suspension from the wafer after withdrawal and before drying. Method 3 (bottom) is similar to the second, except that substrate is immersed in pure water and subsequently emulsion is produce by addition of concentrated emulsion droplets, latter is diluted by copious amounts of water before withdrawing the substrate and drying it.



964

965

966

967

968

969

970

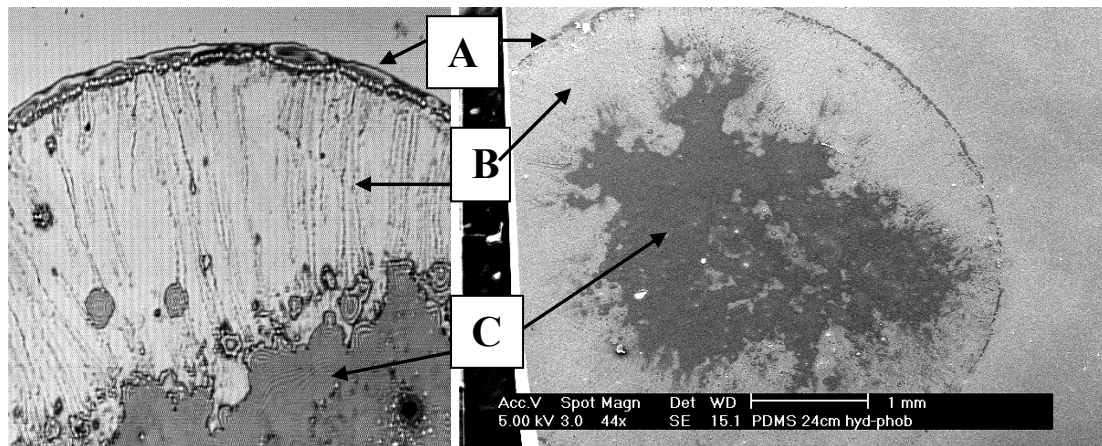
971

972

973

Fig. 12. AFM tapping mode images of PDMS on not treated (high contact angle) silicon wafers, deposited from a drop of concentrated suspension that was subsequently dried. The images are 50 μm frame, and show the result of deposition from an undiluted emulsion drop (50% v/v) followed by air drying (left) and vacuum drying (right).

974



975

976

977

978

979

980

981

982

983

984

985

986

987

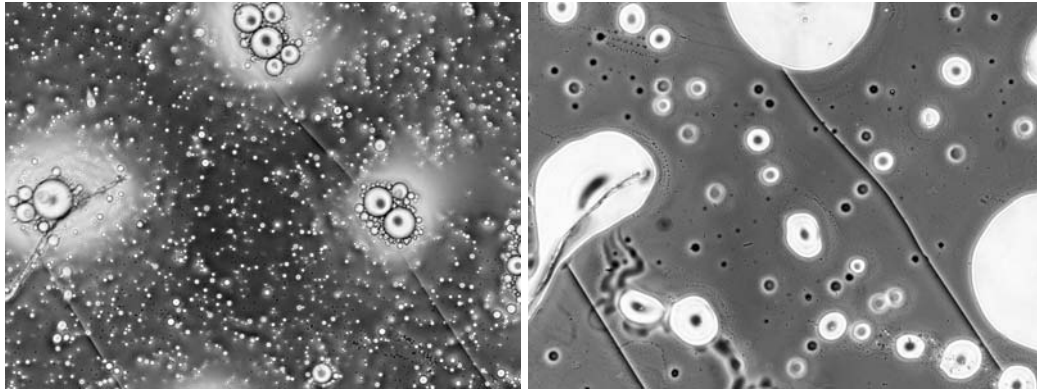
988

989

990

Fig. 13. Optical interference microscope image (left image) of substrate after diluted emulsion drops were vacuum dried on the high contact angle wafer surface. The image, made in reflection using monochromatic light, show constant-thickness interference fringes (Newton's rings) that can be used to measure the height and profile of spread drops. The left-hand image shows the deposition from a drop of emulsion diluted to about 0.025% PDMS. Regions mark respectively the coffee ring (A), a sparse, stringy region(B) and the centre where oil is pooled (C). The right-hand image shows SEM image of similar drop. The scale bars are 1 mm and this image was taken in secondary electron mode.

991
992

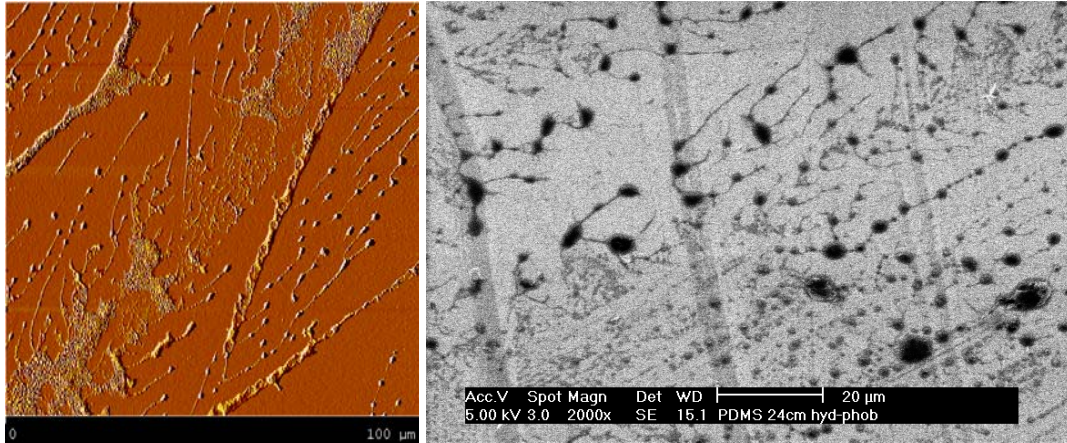


993
994
995

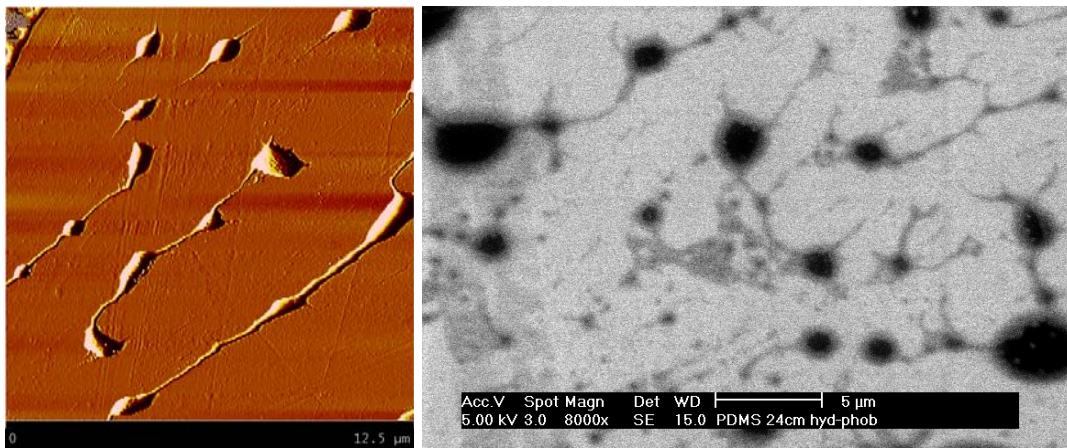
996 **Fig. 14. Droplets of diluted PDMS suspension on hydrophobic substrate when**
997 **draying show increase larger oil spheres which coalesce in to larger oil**
998 **pool.**

999
1000
1001

1002



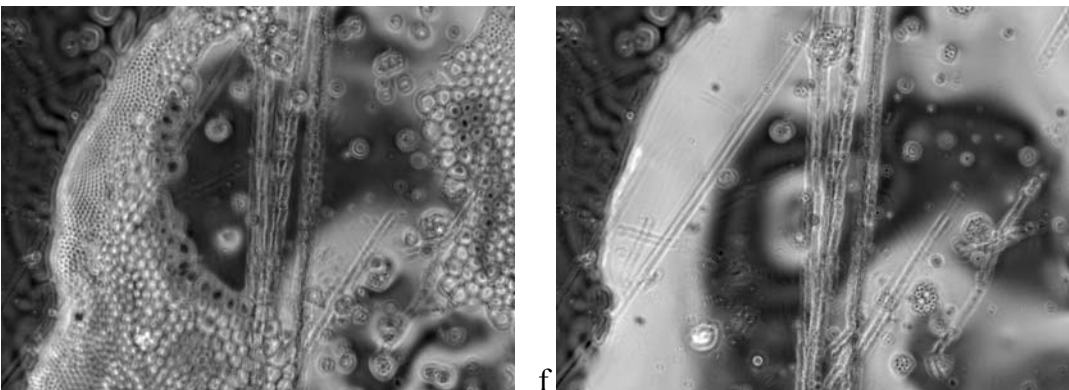
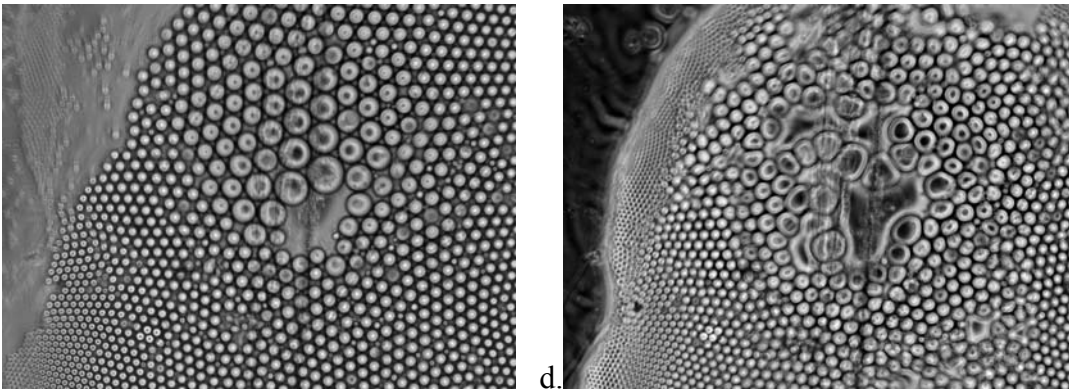
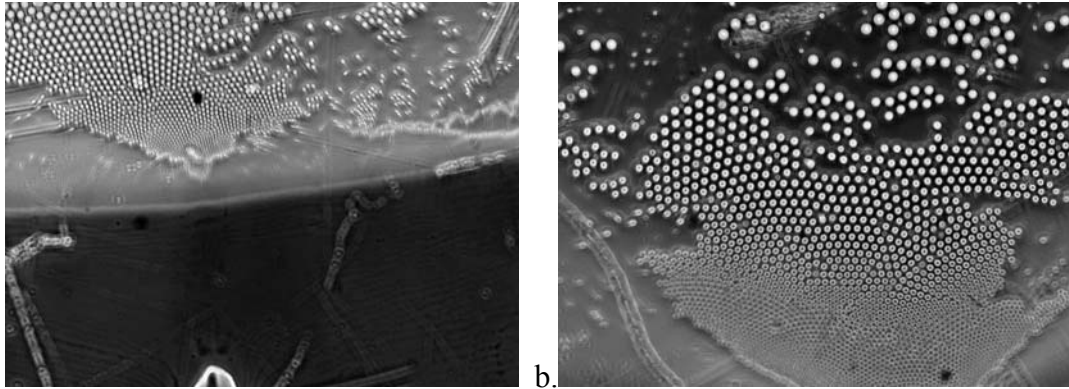
1003
1004



1005
1006
1007
1008
1009
1010
1011
1012
1013
1014
1015

Fig. 15. Comparison between and AFM images (left) SEM images (right) of Region B, showing a clear similarity in the images taken by the different techniques. The scale bars of the secondary electron SEM images are 200 μm (upper right) and 5 μm (lower right), while the AFM images are of 100 μm (upper left) and 12.5 μm (lower left) squares.

1016

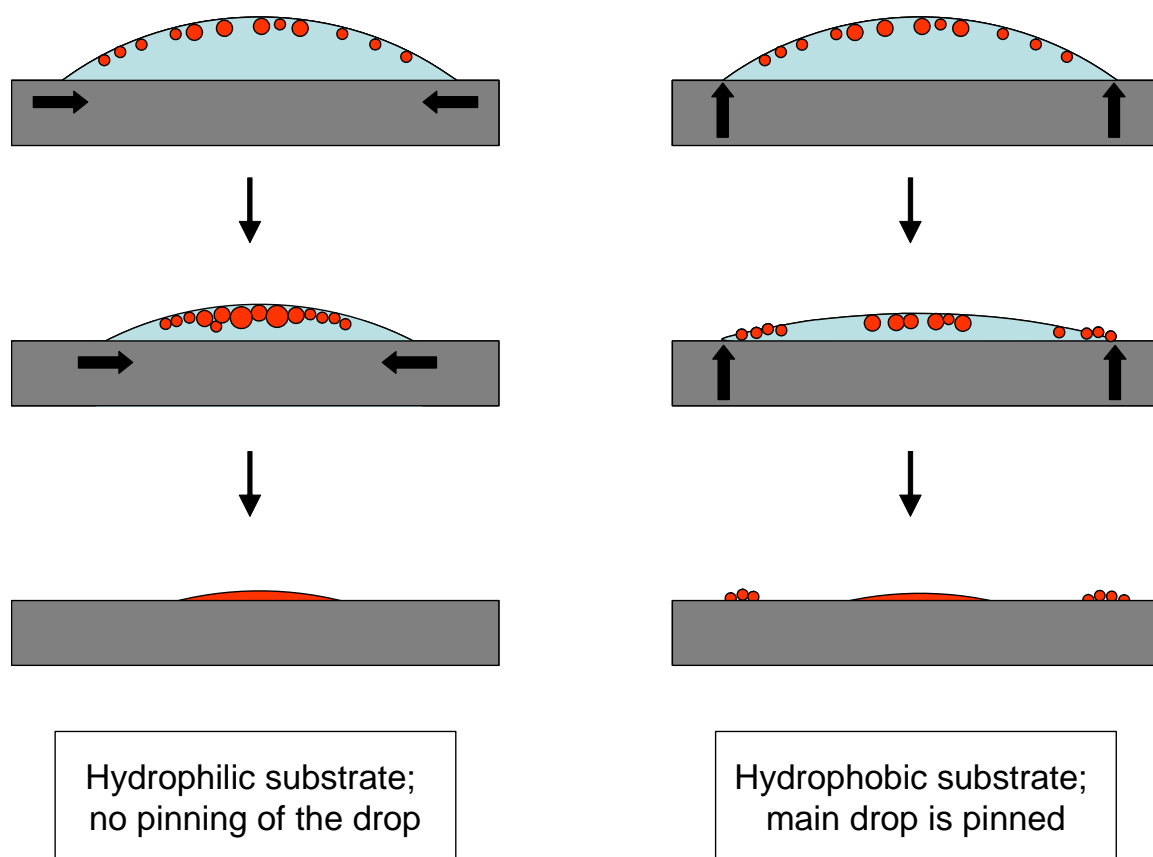


1021
1022
1023
1024
1025
1026
1027
1028
1029
1030
1031
1032
1033
1034
1035
1036

Fig. 16. Optical micrographs of deposition by drying in air of a dilute suspension of 10 μm PDMS emulsion droplets on a hydrophilic surface (freshly-cleaved mica). The width of each image is 220 μm . (a) Near the edge of the main drop which retracts smoothly over the surface as it dries. Emulsion droplets of PDMS are pushed away from the drying edge toward the centre of the main drop. (b) Larger droplets in the distribution are found towards the centre. (c) Large droplets appear at the apex of the drop. It appears that some of the drops must have coalesced, since they are larger than the original 10 μm emulsion droplet size. (d) The large drops at the apex coalesce to form bulk PDMS. (e) A pool of bulk PDMS forms at the apex, and after drying, (f) it is deposited onto the substrate. In this step, remaining emulsion

1037
1038
1039
1040
1041
1042
1043

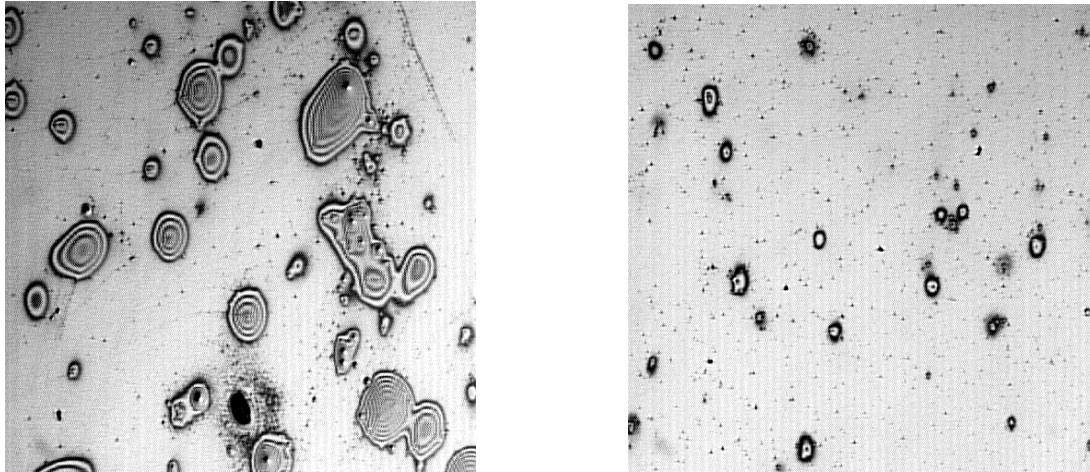
droplets visible off-centre in (e) also coalesce. The whole process from (a) to (f) occupies a few minutes. The rough vertical lines are scratches on the lower surface of the mica. Focus was changed between images as the drop evaporated.



1044
 1045
 1046
 1047
 1048
 1049
 1050
 1051

Fig. 17 Schematic illustration of drying of a drop of suspension (blue) containing emulsion droplets of PDMS (red) with two types of behaviour that we have observed.

1052



1053

1054

1055

1056

1057

1058

1059

1060

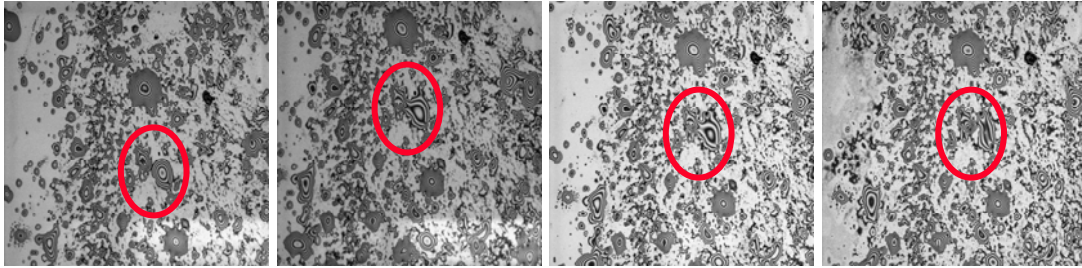
1061

1062

1063

Fig. 18. Optical interference micrographs of 2 mm square regions showing PDMS emulsion droplets deposited on a plasma-treated (hydrophilic) silicon wafer. In this case the suspension wets and spreads over the whole wafer before being vacuum dried. The left-hand images shows deposition from the 0.025% suspension and right-hand side from 0.006% suspension.

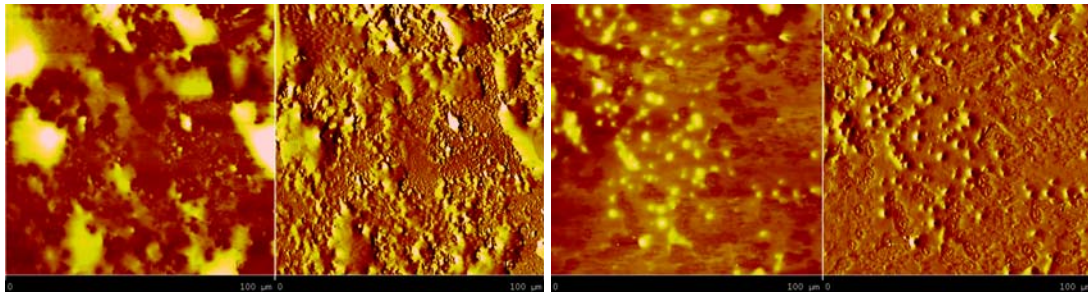
1064



1065
1066
1067
1068
1069
1070
1071
1072
1073
1074
1075
1076
1077
1078

Fig. 19 Optical interference images, each 0.85 mm on the long side, taken at (left to right) 10, 60, 150 and 3600 minutes after drying a 0.025% drop. The upper series shows PDMS on a normal (hydrophobic) wafer and the lower set is for a plasma-treated (hydrophilic) one. Each fringe represents a constant-thickness contour, with contour intervals of $\lambda/2n \approx 240$ nm. Hence the reduction with time of the number of fringes in the same feature of the image shows progressive thinning of PDMS droplets on the surface. Locating the same features in the lower series is not so evident except in the central two images, but the thickness reduction is clear even from these two.

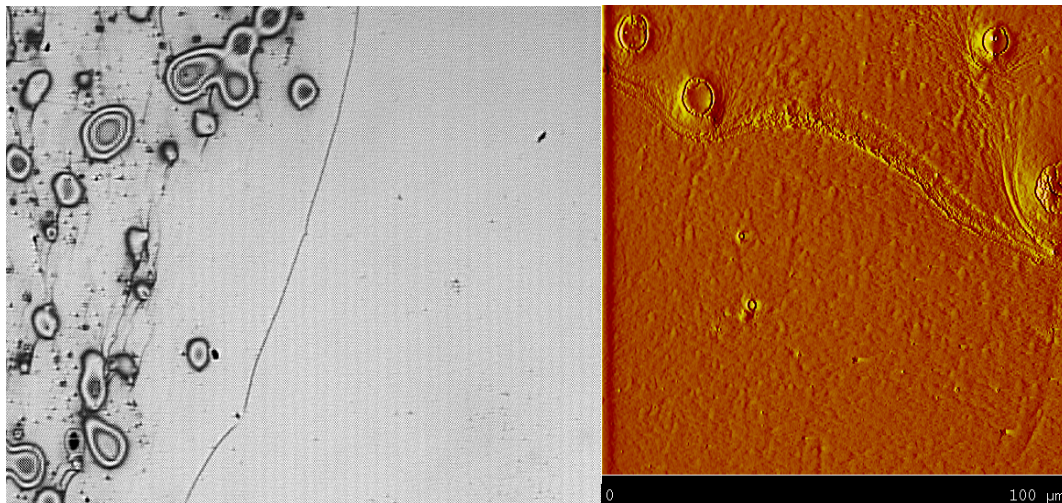
1079



1080
1081
1082
1083
1084
1085
1086
1087
1088
1089

Fig. 20. AFM images of the same samples as in Fig. 21 after 3600 minutes (60 hours). The left-hand pair is for the hydrophobic wafer and the right-hand pair is for the hydrophilic one. An uneven but apparently continuous film is evident on both surfaces.

1090



1091

1092

1093

1094

1095

1096

1097

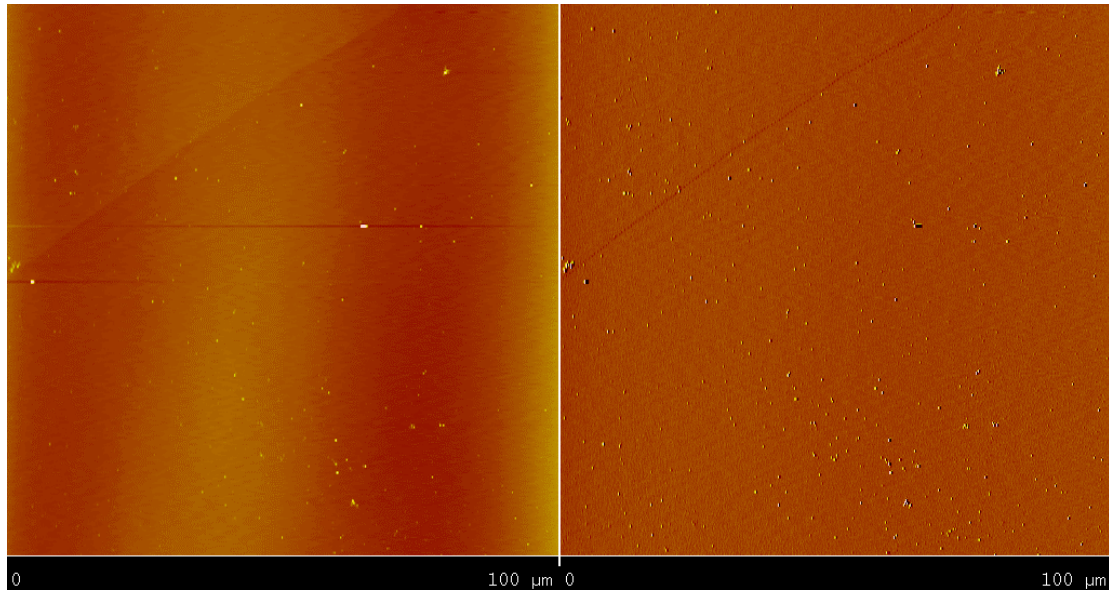
1098

1099

1100

1101

Fig. 21. Optical interference (2 mm square) and AFM images (100 μm square) of PDMS deposited on a hydrophilic silicon wafer by immersion in and withdrawal from a diluted emulsion, then vacuum drying. The left-hand images show deposition from a thick film and the right-hand side from a thin film region (see text).



1102
1103
1104
1105
1106
1107
1108
1109
1110
1111
1112

Fig. 22 AFM images (100 μm square) showing two regions of the Method 3 sample. Droplet deposition is sparse.